



**NAVAL
POSTGRADUATE
SCHOOL**

MONTEREY, CALIFORNIA

THESIS

**AN EXPERIMENTAL STUDY OF ELECTROMAGNETIC
LORENTZ FORCE AND RAIL RECOIL**

by

Michael J. Putnam

December 2009

Thesis Advisor:	William B. Maier II
Co-Advisor:	Peter P. Crooker

Approved for public release; distribution is unlimited

REPORT DOCUMENTATION PAGE			Form Approved OMB No. 0704-0188	
Public reporting burden for this collection of information is estimated to average 1 hour per response, including the time for reviewing instruction, searching existing data sources, gathering and maintaining the data needed, and completing and reviewing the collection of information. Send comments regarding this burden estimate or any other aspect of this collection of information, including suggestions for reducing this burden, to Washington headquarters Services, Directorate for Information Operations and Reports, 1215 Jefferson Davis Highway, Suite 1204, Arlington, VA 22202-4302, and to the Office of Management and Budget, Paperwork Reduction Project (0704-0188) Washington DC 20503.				
1. AGENCY USE ONLY (Leave blank)		2. REPORT DATE December 2009	3. REPORT TYPE AND DATES COVERED Master's Thesis	
4. TITLE AND SUBTITLE An Experimental Study of Electromagnetic Lorentz Force and Rail Recoil			5. FUNDING NUMBERS	
6. AUTHOR(S) Michael J. Putnam				
7. PERFORMING ORGANIZATION NAME(S) AND ADDRESS(ES) Naval Postgraduate School Monterey, CA 93943-5000			8. PERFORMING ORGANIZATION REPORT NUMBER	
9. SPONSORING /MONITORING AGENCY NAME(S) AND ADDRESS(ES) N/A			10. SPONSORING/MONITORING AGENCY REPORT NUMBER	
11. SUPPLEMENTARY NOTES The views expressed in this thesis are those of the author and do not reflect the official policy or position of the Department of Defense or the U.S. Government.				
12a. DISTRIBUTION / AVAILABILITY STATEMENT Approved for public release; distribution is unlimited			12b. DISTRIBUTION CODE	
13. ABSTRACT (maximum 200 words) Understanding whether recoil forces are seated in the rails of any electromagnetic launch technology, including railguns, is critical for efficient development and design. Several theoretical and experimental researchers have produced multiple published papers characterizing rail recoil. These papers are not definitive and often conflict. An experiment has been developed that allows for the simultaneous measurements of the quasi-static Lorentz force on the armature and rail recoil. The primary challenge in quantifying these forces is removing the mechanical coupling required to construct the necessary circuit while maintaining electrical connectivity. Liquid metal Ga/In eutectic was used to conduct electricity while mechanically decoupling the rails from the rest of the circuit. Force measurements show that the force on the armature increases as the square of the current while the indicated reaction force on the rails is an artifact of the experiment. These recoil forces measured <1% of the force on the armature. We conclude that the recoil, or corresponding equal and opposite reaction force to the force on the armature, is not seated in the rails.				
14. SUBJECT TERMS Railgun, Railgun recoil, Lorentz force, eutectic			15. NUMBER OF PAGES 71	
			16. PRICE CODE	
17. SECURITY CLASSIFICATION OF REPORT Unclassified	18. SECURITY CLASSIFICATION OF THIS PAGE Unclassified	19. SECURITY CLASSIFICATION OF ABSTRACT Unclassified	20. LIMITATION OF ABSTRACT UU	

THIS PAGE INTENTIONALLY LEFT BLANK

Approved for public release; distribution is unlimited

**AN EXPERIMENTAL STUDY OF ELECTROMAGNETIC LORENTZ FORCE
AND RAIL RECOIL**

Michael J. Putnam
Lieutenant, United States Navy
B.S., University of North Florida, 2003

Submitted in partial fulfillment of the
requirements for the degree of

MASTER OF SCIENCE IN APPLIED PHYSICS

from the

**NAVAL POSTGRADUATE SCHOOL
December 2009**

Author: Michael J. Putnam

Approved by: William B. Maier II
Thesis Advisor

Peter P. Crooker
Co-Advisor

Andres Larraza
Chairman, Department of Physics

THIS PAGE INTENTIONALLY LEFT BLANK

ABSTRACT

Understanding whether recoil forces are seated in the rails of any electromagnetic launch technology, including railguns, is critical for efficient development and design. Several theoretical and experimental researchers have produced multiple published papers characterizing rail recoil. These papers are not definitive and often conflict. An experiment has been developed that allows for the simultaneous measurements of the quasi-static Lorentz force on the armature and rail recoil. The primary challenge in quantifying these forces is in removing the mechanical coupling required to construct the necessary circuit while maintaining electrical connectivity. Liquid metal Ga/In eutectic was used to conduct electricity while mechanically decoupling the rails from the rest of the circuit. Force measurements show that the force on the armature increases as the square of the current while the indicated reaction force on the rails is an artifact of the experiment. These recoil forces measured <1% of the force on the armature. We conclude that the recoil, or corresponding equal and opposite reaction force to the force on the armature, is not seated in the rails.

THIS PAGE INTENTIONALLY LEFT BLANK

TABLE OF CONTENTS

I.	INTRODUCTION	1
A.	MOTIVATION	1
B.	OBJECTIVE	2
C.	BACKGROUND	2
II.	EXPERIMENTAL SETUP	5
A.	PREVIOUS RESEARCH	5
B.	COMPONENTS	5
1.	The Rails	5
2.	Pendulum Suspension	6
3.	Armature and Eutectic	7
4.	Power Supply, Switching, and Resistance	9
5.	Splitting the Rails	11
6.	Instrumentation	13
III.	EXPERIMENTAL PROCEDURE	17
A.	SCOPE	17
B.	RECORDING LORENTZ FORCE AND RECOIL	17
C.	SPLITTING THE RAILS	18
IV.	EXPERIMENTAL RESULTS	19
A.	SIMULTANEOUS LORENTZ AND RECOIL FORCES	19
B.	SPLIT RAIL MEASUREMENTS	25
1.	Armature Lorentz Force and Recoil on the Muzzle Half Rail	25
2.	Forces Between the Rail Halves	27
C.	SUMMARY	29
APPENDIX	31
1.	LORENTZ FORCE AND RECOIL	31
2.	SPLIT RAILS—LORENTZ FORCE AND MUZZLE HALF RECOIL ..	37
3.	SPLIT RAILS—OPPOSING FORCES ON EACH RAIL HALF	45
LIST OF REFERENCES	49
INITIAL DISTRIBUTION LIST	53

THIS PAGE INTENTIONALLY LEFT BLANK

LIST OF FIGURES

Figure 1.	Schematic illustration of railgun operation [From 29].....	3
Figure 2.	Copper rails and armature.....	5
Figure 3.	Pendulum suspension system-not to scale, [From 30].....	6
Figure 4.	Rail/armature interface.....	8
Figure 5.	3D translation system.....	8
Figure 6.	Schematic of model railgun circuit (not to scale).....	9
Figure 7.	Graphite plate resistor.....	10
Figure 8.	Meidensha 50 kA vacuum interrupter and breech electrical connection.....	11
Figure 9.	Split rails.....	12
Figure 10.	Rail tabs submerged in eutectic.....	12
Figure 11.	LC305-25 load cell.....	13
Figure 12.	Ammeter shunt with leads routed to USB-6211 DAQ.....	14
Figure 13.	NI USB-6211 DAQ connected to laptop.....	15
Figure 14.	SR560 low noise preamplifiers connected to USB-6211.....	16
Figure 15.	Instrumentation flow chart.....	16
Figure 16.	Lorentz force armature load cell (a), recoil force load cell (b).....	17
Figure 17.	Load cells set up for split rails.....	18
Figure 18.	Armature Lorentz force and rail recoil force for 1.2 kA pulse.....	21
Figure 19.	Armature Lorentz forces and rail recoil forces for 1.2 kA and 2.5 kA pulses.....	22
Figure 20.	Armature Lorentz force and steady state rail recoil vs current.....	24
Figure 21.	Split rails-armature Lorentz force and rail recoil force for 1.8 kA pulse.....	26
Figure 22.	Split rail-Opposing rail forces for 2 kA current pulse.....	28
Figure 23.	Armature Lorentz force and rail recoil force for 1.2 kA pulse.....	31
Figure 24.	Armature Lorentz force and rail recoil force for 1.5 kA pulse.....	32
Figure 25.	Armature Lorentz force and rail recoil force for 1.7 kA pulse.....	33
Figure 26.	Armature Lorentz force and rail recoil force for 1.8 kA pulse.....	34
Figure 27.	Armature Lorentz force and rail recoil force for 2.6 kA pulse.....	35

Figure 28.	Armature Lorentz force and rail recoil force for 2.7 kA pulse.....	36
Figure 29.	Split rail–armature Lorentz force and recoil force for 0.7 kA pulse.....	37
Figure 30.	Split rail–armature Lorentz force and recoil force for 1.2 kA pulse.....	38
Figure 31.	Split rail–armature Lorentz force and recoil force for 1.3 kA pulse.....	39
Figure 32.	Split rail–armature Lorentz force and recoil force for 1.3 kA pulse.....	40
Figure 33.	Split rail–armature Lorentz force and recoil force for 1.4 kA pulse.....	41
Figure 34.	Split rail–armature Lorentz force and recoil force for 1.4 kA pulse.....	42
Figure 35.	Split rail–armature Lorentz force and recoil force for 1.9 kA pulse.....	43
Figure 36.	Split rail–armature Lorentz force and recoil force for 2 kA pulse.....	44
Figure 37.	Split rail–opposing rail forces for 1.1 kA current pulse.....	45
Figure 38.	Split rail–opposing rail forces for 1.2 kA current pulse.....	46
Figure 39.	Split rail–opposing rail forces for 1.4 kA current pulse.....	47

LIST OF TABLES

Table 1.	Peak rail recoil force measurements.....	23
Table 2.	Steady-state rail recoil forces.....	23

THIS PAGE INTENTIONALLY LEFT BLANK

ACKNOWLEDGMENTS

I would like to thank Professor Bill Maier for his guidance and endless support. This project was made possible by his previous work with Matthew Schroeder.

I would like to thank Professor Pete Crooker for his tremendous teaching ability. Without his assistance, I would still be toiling away and this research project would not have been the same.

I must recognize Don Snyder and Gene Morris who are the technicians behind the scenes that make everything happen in the NPS railgun lab. Their help was instrumental in every phase of this research project.

This work was supported by the Office of Naval Research and their Electromagnetic Railgun Program.

THIS PAGE INTENTIONALLY LEFT BLANK

I. INTRODUCTION

A. MOTIVATION

For over 200 years, electromagnetic forces have been extensively researched. During 1802, Gian Domenico Romagnosi noticed that a magnetic needle deflected when electricity from a crude battery was turned on and off [1]. Less than 20 years later, Hans Christian Oersted independently discovered the same phenomenon, and through further experiments, deduced that a current carrying wire produces a magnetic field [2]. This electric force was put to use in the first electric gun by Joachim Hansler in 1844 [3], some 48 years before Lorentz introduced his force equation in 1892 [4].

Even though the Lorentz force has been known for well over 100 years, its corresponding reaction force is still a topic of controversy. Numerous theoretical and experimental researchers have tackled this issue, with a wide variety of results [5]-[27]. An experiment by Graneau [28], led him to conclude that there are longitudinal recoil forces seated in the rails. Witalis [26], asserts that relativistic recoil forces are exerted on the rails in a direction parallel to the rails [26].

Allen and Jones [5,6] state that Graneau is incorrect. They claim railgun rails will not recoil, but instead recoil occurs at the breech due to reflected waves, which create "electric pressure" via "electromagnetic momentum." Also, Marshall and Woods [16] rebut Witalis's work by

combining theory with empirical observations from the Canberra railgun. They conclude recoil forces are not seated in the rails.

Sadedin suggests that momentum can be conserved in railguns by modeling recoil forces as a gas pressure [22]. Graneau refutes this notion by stating that the Lorentz force law fails to predict where recoil is seated [18]. Clearly there is room for experiment to resolve this controversy.

B. OBJECTIVE

The focus of this thesis was to determine if electromagnetic recoil forces are seated in the rails. Experimental research was conducted to produce quantitative evidence that will definitively answer this question. It should be noted that the scope of this thesis does not include determining where else recoil forces may be seated. Specifically, this experiment quasi-statically measures the force that accelerates the armature and compares that with the measured recoil force.

C. BACKGROUND

Railguns operate through the interaction of flowing electrons in the armature with the magnetic fields produced by electric current in the rails. This interaction produces what is called the Lorentz force,

$$F = \frac{1}{2} L' I^2 \tag{1}$$

which is exerted on the armature and accelerates it down the barrel. In this equation, L' is the inductance gradient per unit length of the rail pair, and I is the

current flowing through the rails and armature. Equation (1) is widely accepted as the force on railgun armatures [29]. Figure 1 illustrates how the Lorentz force accelerates an armature.

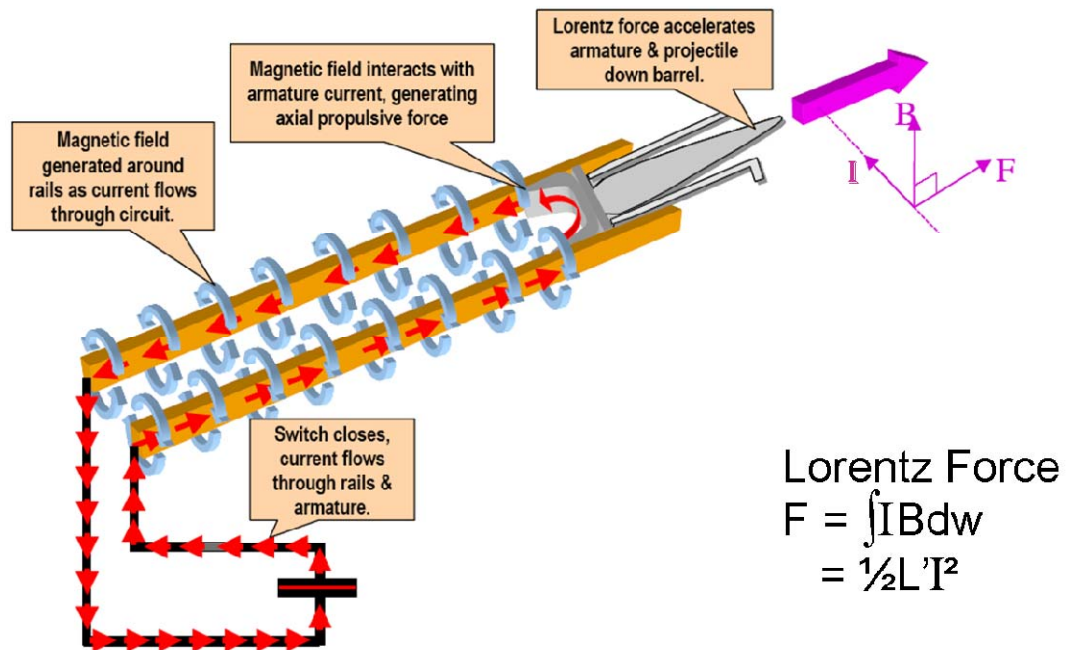


Figure 1. Schematic illustration of railgun operation (From [29])

THIS PAGE INTENTIONALLY LEFT BLANK

II. EXPERIMENTAL SETUP

A. PREVIOUS RESEARCH

This thesis is a continuation of LT Matthew Schroeder's research [30]. His work included the design and construction of the experimental apparatus used to conduct the research in this thesis. New modifications will be specifically mentioned during the overview of the complete experimental setup.

B. COMPONENTS

1. The Rails

Figure 2 shows a picture of the setup taken from the muzzle end. Fabricated from copper bar stock, the rails are approximately 3 cm wide by 0.5 cm tall. The separation between the rails is about 5 cm and they are 2 m long.

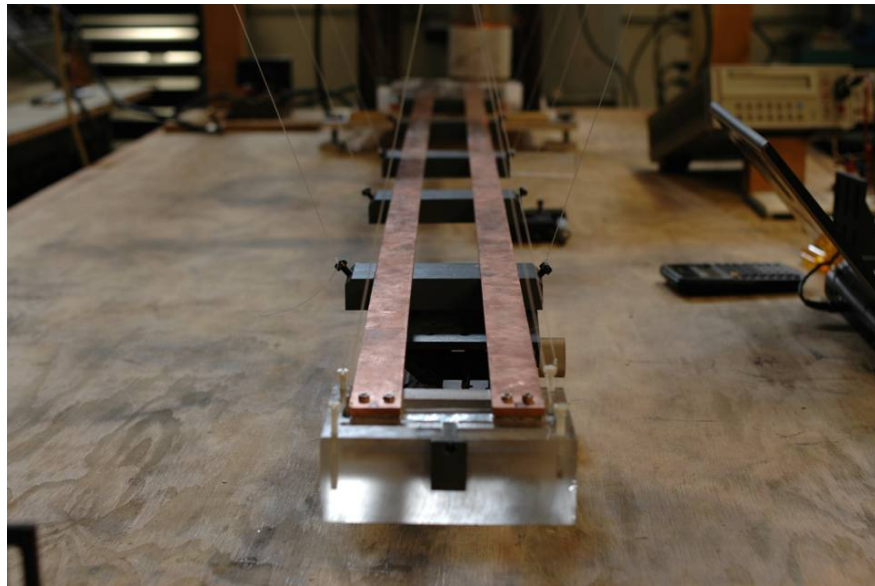


Figure 2. Copper rails and armature

2. Pendulum Suspension

Five polyvinylchloride (PVC) blocks supported the rails. These blocks were suspended from monofilament line forming a 'V' shaped pendulum. The line was attached to two parallel 8 ft long 2 X 4 in wood beams. Figure 3 displays the suspended rails, which are free to move along the longitudinal axis of the rails. The design dimensions are given in Figure 3. The two top beams that the pendulum lines hang from are 8 ft long 2 X 4 in wood boards. The distance between the two top beams is 4 ft.

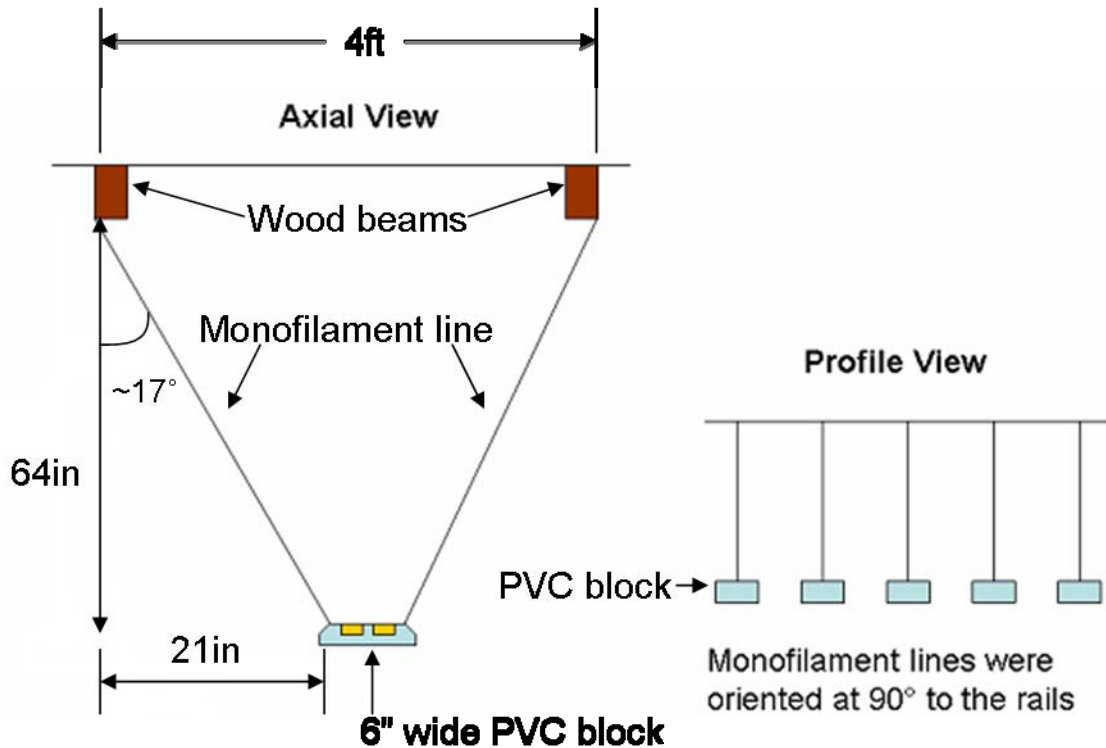


Figure 3. Pendulum suspension system-not to scale,
(From [30])

3. Armature and Eutectic

The armature consisted of a suspended plastic block with liquid metal Gallium/Indium eutectic in a 2 cm deep polycarbonate reservoir. Copper tabs, which measured 1.8 cm deep, were attached to the rails and dipped into the eutectic. Shown in Figure 4, this interface removed most of the mechanical coupling between the rails and the armature while still allowing current flow. The inability of the fluid to sustain a shear force allowed the rail and armature to move independently of one another. The armature was suspended from four corners by monofilament line which connected to a swivel 12 in above. The swivel was connected by a single line to the three dimensional translation system pictured in Figure 5. These optical mounts contained micrometer adjustments, which provided for precise positioning of the armature in relation to the rails. Proper adjustment ensured no physical contact between the rails and the armature block.

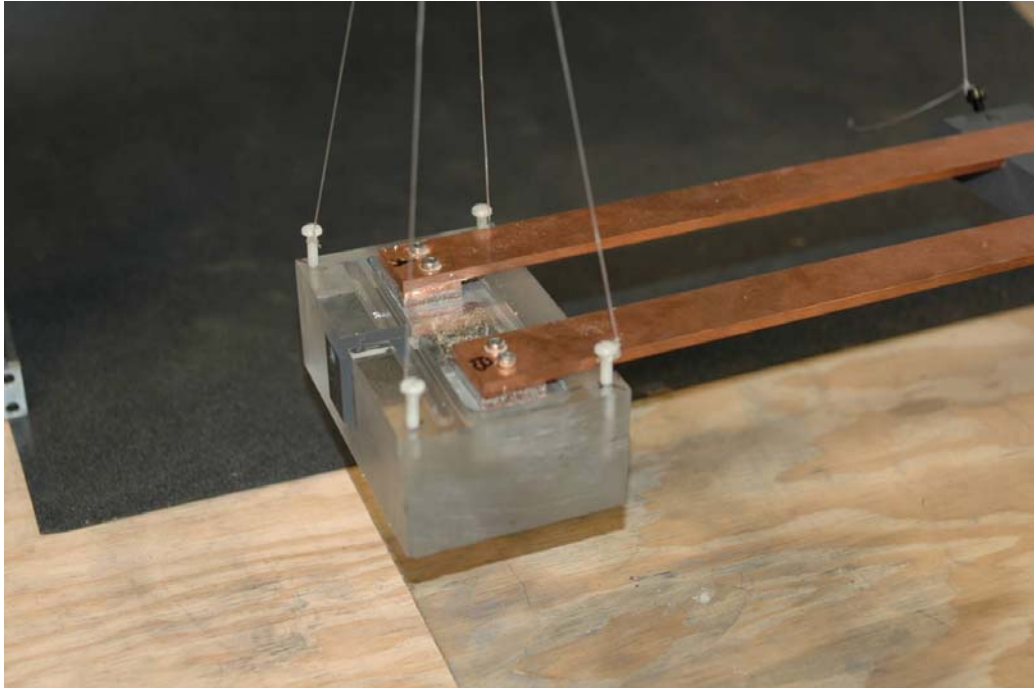


Figure 4. Rail/armature interface



Figure 5. 3D translation system

4. Power Supply, Switching, and Resistance

The power supply consisted of a large variable resistor in series with four Autolite 96 Platinum car batteries connected in parallel as shown in the schematic of Figure 6. Higher currents were obtained by connecting four more batteries in parallel, thereby lowering the combined internal resistance. Currents between 800 A and 2.7 kA were used.

The high currents required a variable resistor which was capable of dissipating the corresponding I^2R losses. The led to the use of a large stack of graphite plates as a variable resistor. The number of plates and the compression on them could be changed to control how much current flowed through the rails. The graphite plates were 0.5 cm thick and there were 100 plates total. Two copper plates were moved to alter the number of graphite plates in the current path. Small partial turns on the compression wheel adjusted the resistance by micro-ohms. Figure 7 shows the compressible graphite plates and the two copper plates.

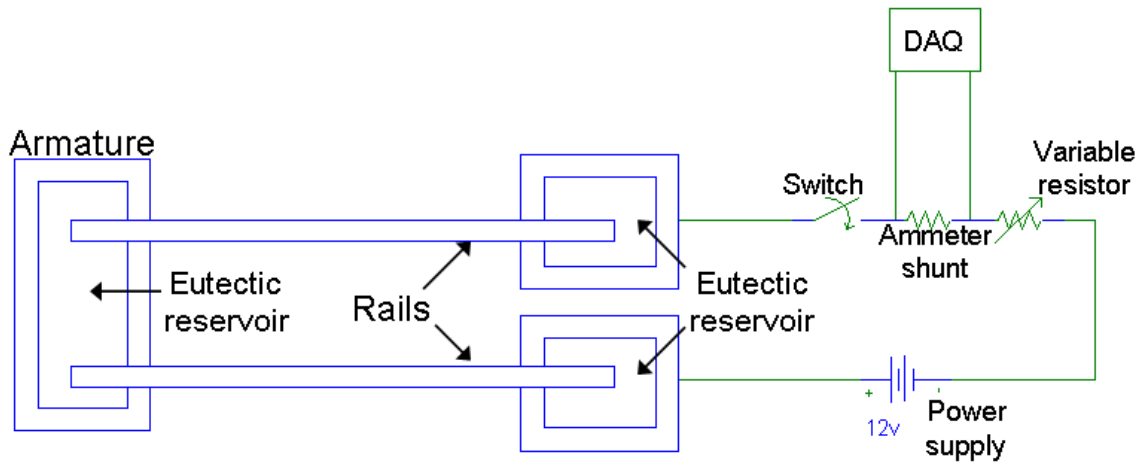


Figure 6. Schematic of model railgun circuit (not to scale)

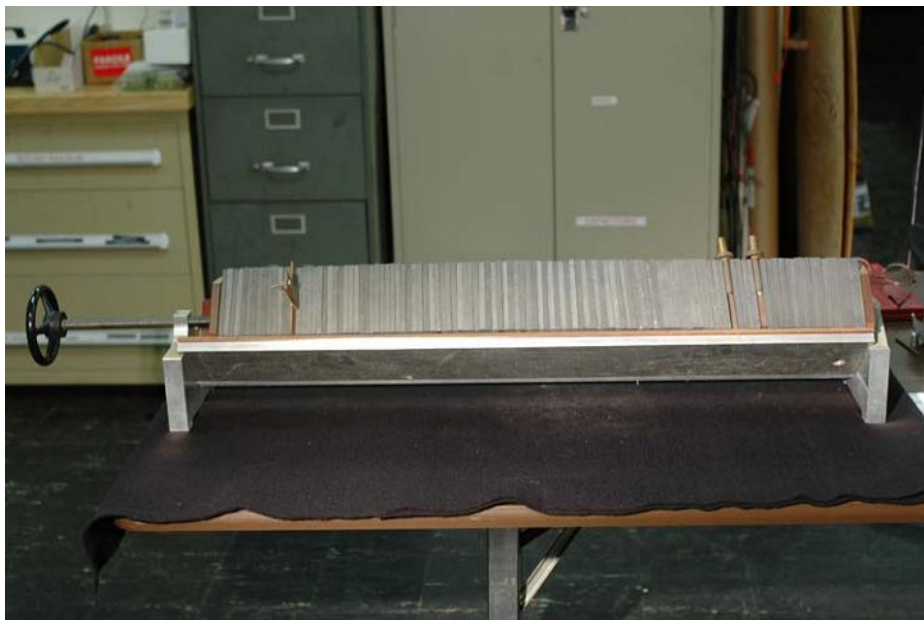


Figure 7. Graphite plate resistor

Current was turned on and off using the high current industrial switch shown in Figure 8. The switch was vacuum sealed and pneumatically actuated. A toggle switch was wired to control flow of an inert gas to the actuator. The actuator took approximately 1 s to close the switch, but opened in a small fraction of a second.

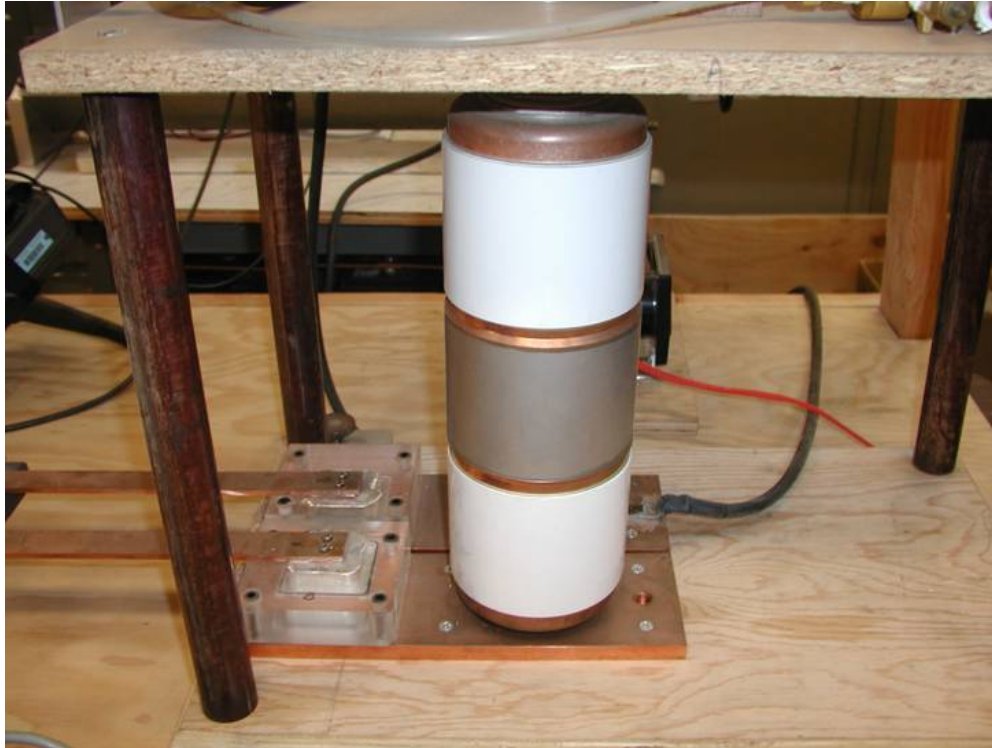


Figure 8. Meidensha 50 kA vacuum interrupter and breech electrical connection

Liquid metal eutectic electrically coupled the rails to the bus bars, as shown in Figure 8. The Gallium-Indium eutectic had relatively small viscosity, but was highly conductive. Since the eutectic was unable to sustain a shear force and the rails were suspended, the rails were entirely free to move. The pendulum suspension system did, however, provide a small restoring force measured at approximately 0.025 N.

5. Splitting the Rails

After initial testing was complete, it was deemed necessary to split the rails (explained in Chapter III, section C). The rails were cut in the middle at 1 m, and then each new end had copper tabs attached, just as at the breech

and muzzle ends. A polycarbonate block had two reservoirs filled with eutectic. The block was raised using a lab jack until the tabs were sufficiently submerged to complete the circuit's electrical connectivity. Figures 9 and 10 show different views of the split rails, ready to energize.

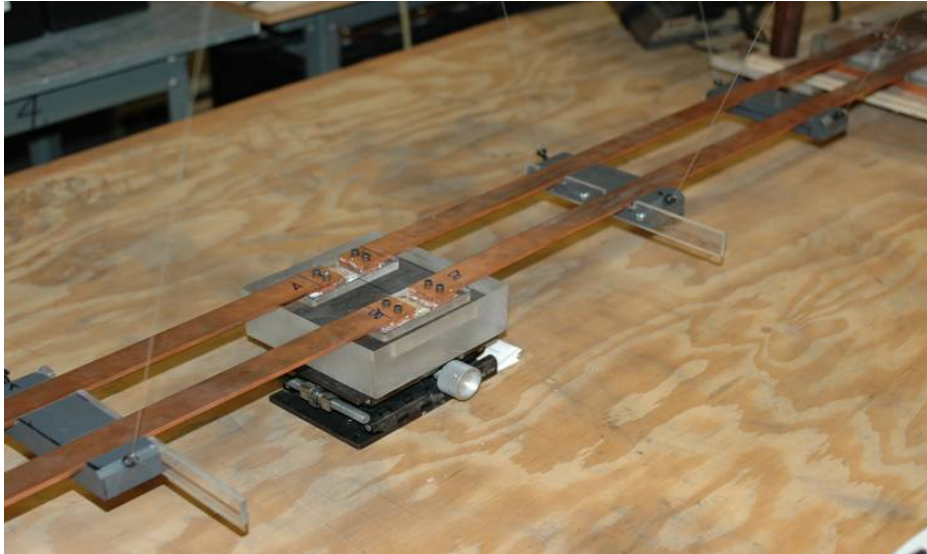


Figure 9. Split rails

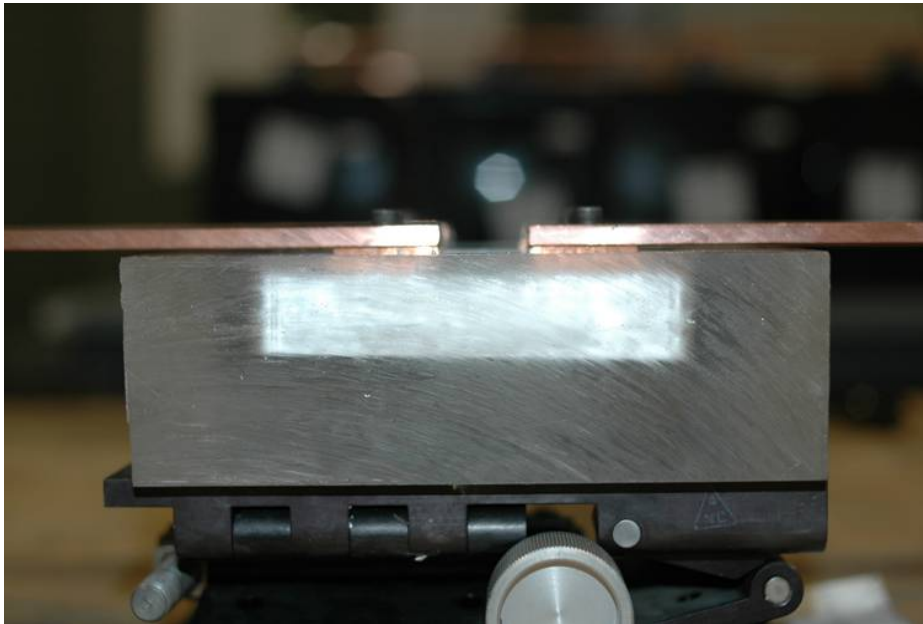


Figure 10. Rail tabs submerged in eutectic

6. Instrumentation

Measurement of forces was accomplished with strain gauges. The LC305-25, by Omega Engineering, is a 2 in diameter miniature stainless steel compression load cell, shown in Figure 11. These gauges were fixed to optical mounts, which were fastened to the table. The micrometer slide provided precise positioning. Each LC305-25 required a 10 v power source to operate, and produced 193 μv per Newton of force. The deflection of the load cell for the magnitude of forces being measured was less than 0.001 in or 25 μm .

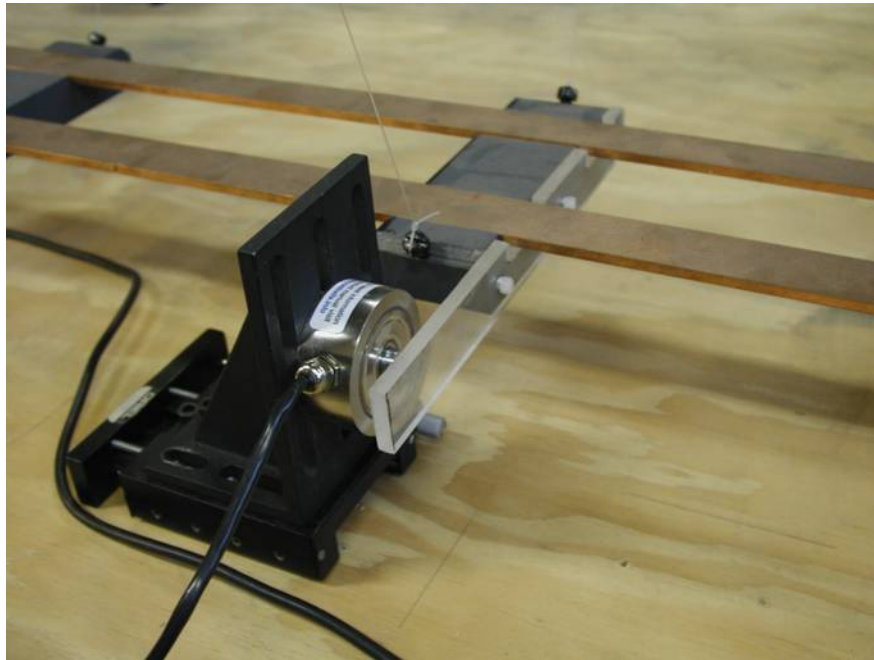


Figure 11. LC305-25 load cell

Current through the rails was determined by use of an ammeter shunt. The shunt has a known resistance ($62.5 \mu\Omega$), and the voltage drop across the shunt was input to the data acquisition converter (DAQ) for analog-to-digital conversion. This data was then sent via USB to a PC for

Labview to process and display continuous real-time current readings. (Schroeder's research used an analog voltmeter and calculations to find the current.) Figure 12 shows the ammeter shunt with leads.

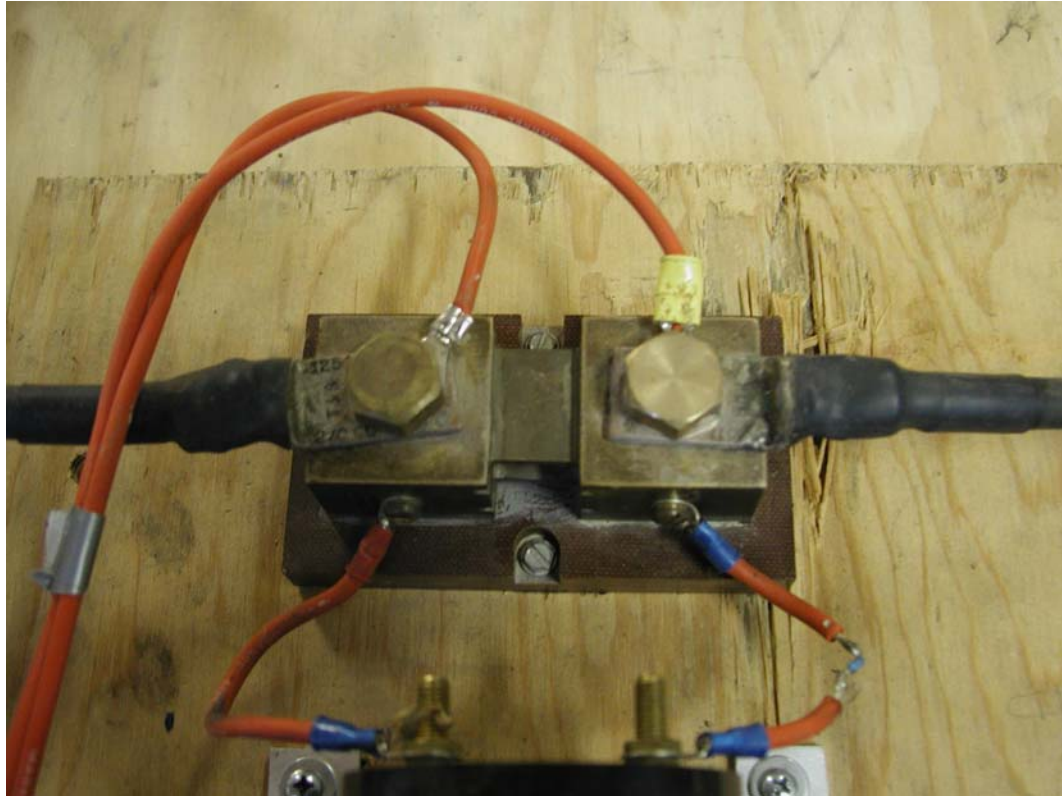


Figure 12. Ammeter shunt with leads routed to USB-6211 DAQ

During previous research [7], the meter of choice was an Omega Engineering DP41-B-4R-A-EI 1/8 DIN ultra-high performance meter, which provided peak force measurements. The meter used in this research was the superior National Instruments USB-6211 DAQ. The 6211 provided real-time continuous data collection via 16 analog inputs with 16 bits of resolution at a sample rate of up to 250 kS/s. The USB-6211, shown in Figure 13, connects via USB to a laptop, and is utilized with a Labview program.

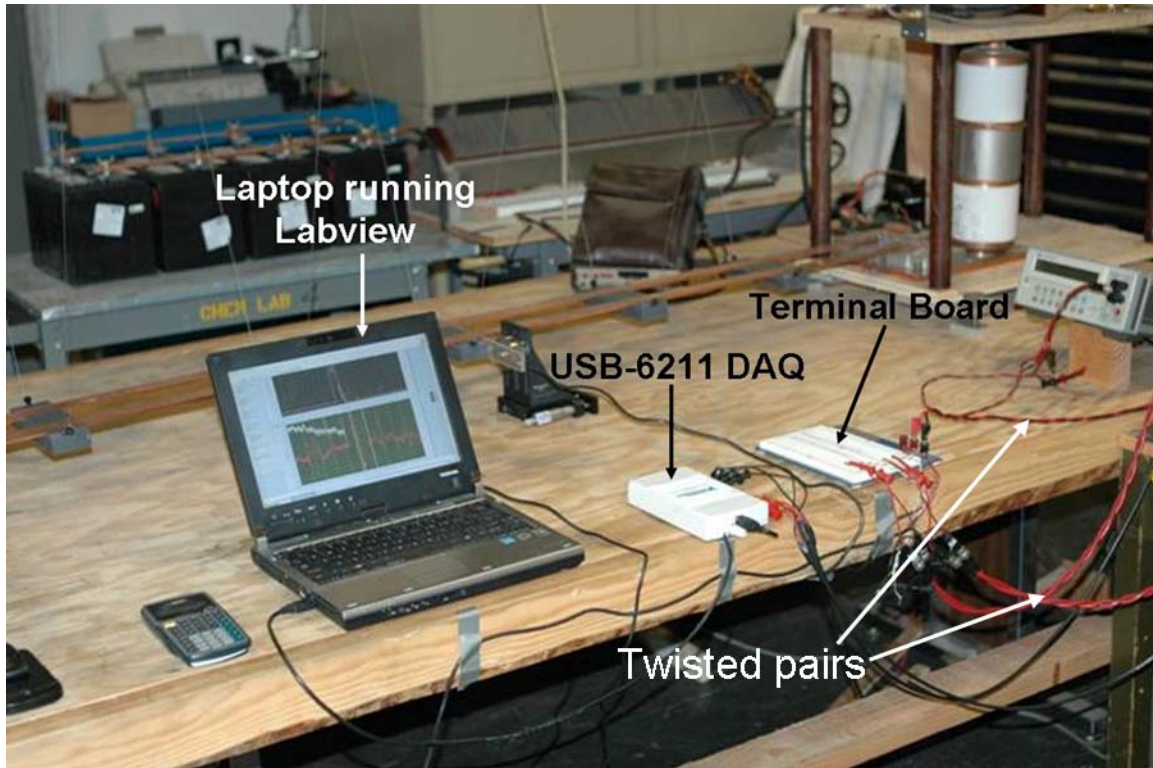


Figure 13. NI USB-6211 DAQ connected to laptop

The use of two Stanford Research Systems model SR560 Low Noise Preamplifiers were needed since forces on the order of 0.01 N produced voltage signals of approximately 2 μv . These preamps provided noise filtering and amplification prior to input into the USB-6211 DAQ. A differential input connection was required with twisted pair wire routing to minimize noise and interference, as shown in Figure 14. The functional flow of all instrumentation is displayed in Figure 15.

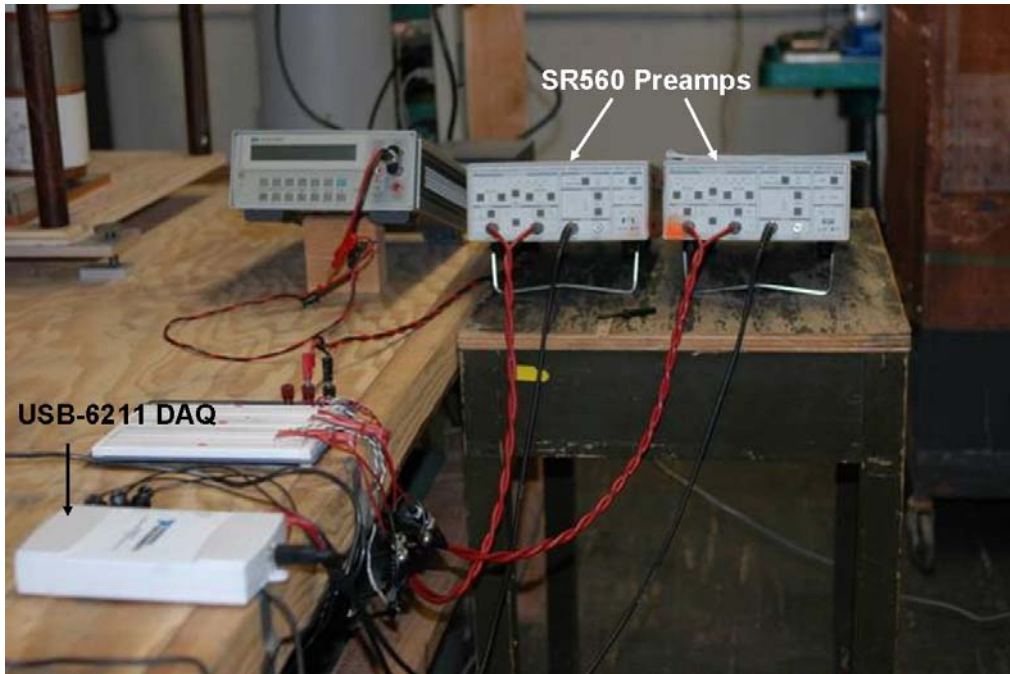


Figure 14. SR560 low noise preamplifiers connected to USB-6211

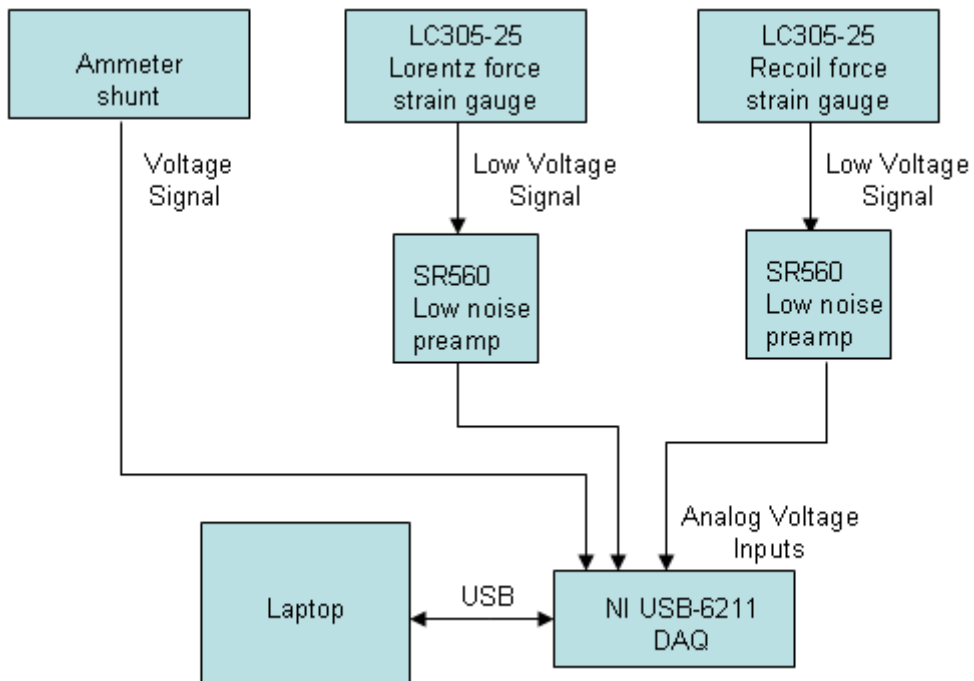


Figure 15. Instrumentation flow chart

III. EXPERIMENTAL PROCEDURE

A. SCOPE

The objective of this experiment was to determine if recoil forces were seated in the rails. This was attacked in two phases: 1) simultaneous measurement of the Lorentz force and rail recoil, and 2) splitting the rails to further examine the possibility of forces seated in the rails.

B. RECORDING LORENTZ FORCE AND RECOIL

To capture these forces, one load cell was mounted in front of the armature, as shown in Figure 16(a). A second load cell was positioned to detect recoil forces as shown in Figure 16(b).



Figure 16. Lorentz force armature load cell (a),
recoil force load cell (b)

The circuit was energized by activating the toggle switch, which initiated the closing of the vacuum interrupter. After approximately 4 seconds, the circuit was de-energized. Data recording was initiated approximately 3 seconds before the circuit was energized, and ran for 10 seconds.

C. SPLITTING THE RAILS

After the rails failed to recoil at currents as high as 2.6 kA and Lorentz forces above 1.5 N, the rails were split to investigate for internal stress. It was not believed, but thought possible, that there might be a force on the rails from the breech, which could cancel recoil forces. Splitting the rails properly would show if these forces existed.

After the rails were split, simultaneous force measurements were taken from the armature and the adjacent muzzle half of the rails, for different current levels. The same procedure previously mentioned for recording data was utilized. To determine if the split rails pushed toward each other, two load cells were placed accordingly, as shown in Figure 17. However, the rails were instead discovered to push apart with a small force as discussed in the Chapter IV. The load cells were repositioned accordingly to capture this force.

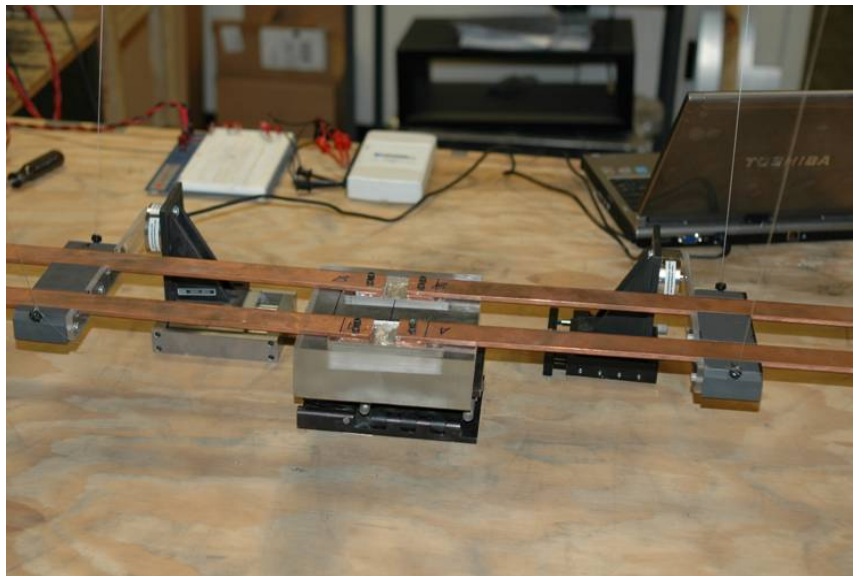


Figure 17. Load cells set up for split rails

IV. EXPERIMENTAL RESULTS

A. SIMULTANEOUS LORENTZ AND RECOIL FORCES

Force measurements were recorded for current levels up to 2700 amps. Figure 18 shows a 1200 amp current pulse and the corresponding forces produced. At 1200 amps, the Lorentz force magnitude is approximately 10 times greater than the peak recoil reading, and 30 times greater than the steady-state recoil. The data shows that higher currents resulted in recoil forces of the same magnitude, as seen in Figure 19. These recoil readings are interpreted as artifacts of the experiment. For larger currents, the I^2R losses produced enough heat to raise the copper's resistance. This created the declining current levels seen in many current pulses.

Additional artifacts are labeled in Figure 18 for explanation. Table vibrations occurred whenever the high current switch was opened or closed. The load cells detected all vibrations, since they were adjusted to be in contact, or preloaded. When preloaded, the force reading was set to zero via Labview. Upon separation, this caused the load cell to produce a negative force reading, or preload release. To measure a force, the load cell had to be in contact with the rail support or armature. This contact between the stainless steel load cell and hard plastic created bouncing if the two separated and came back together. These bounces appeared as force oscillations on the graphs.

As current began to flow, there were transient mechanical oscillations in the rails and eutectic, which

caused the recoil peak. While current flowed through the eutectic in the armature, the liquid metal was pushed forward by the Lorentz force. When current stopped flowing, the eutectic flowed back and the armature would swing back and bump the rails. This caused the large peaks in recoil after current flow had stopped.

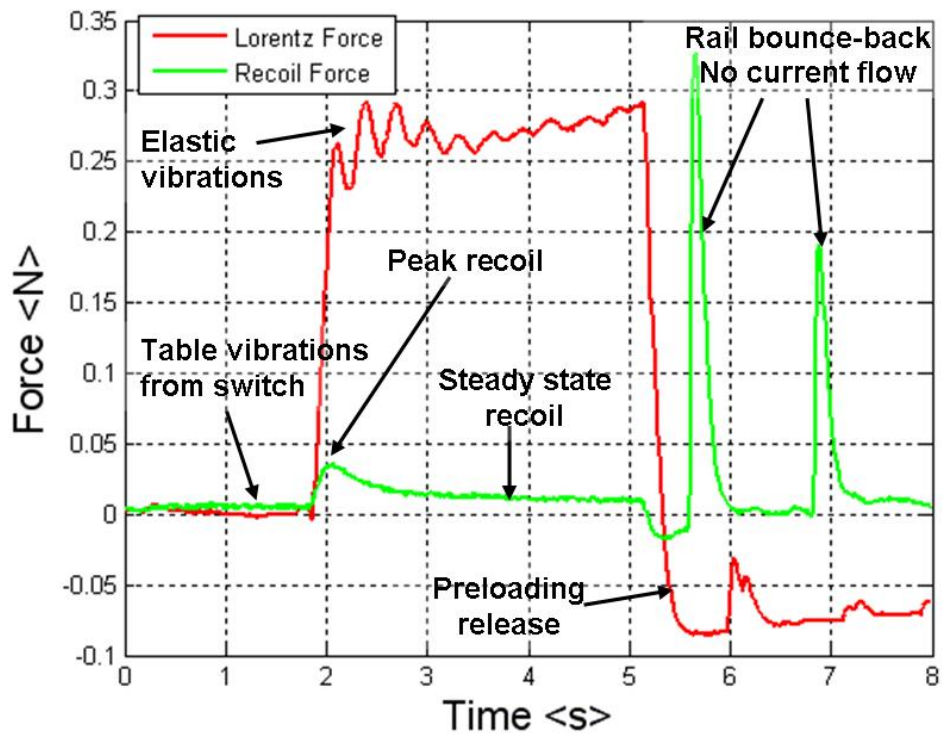
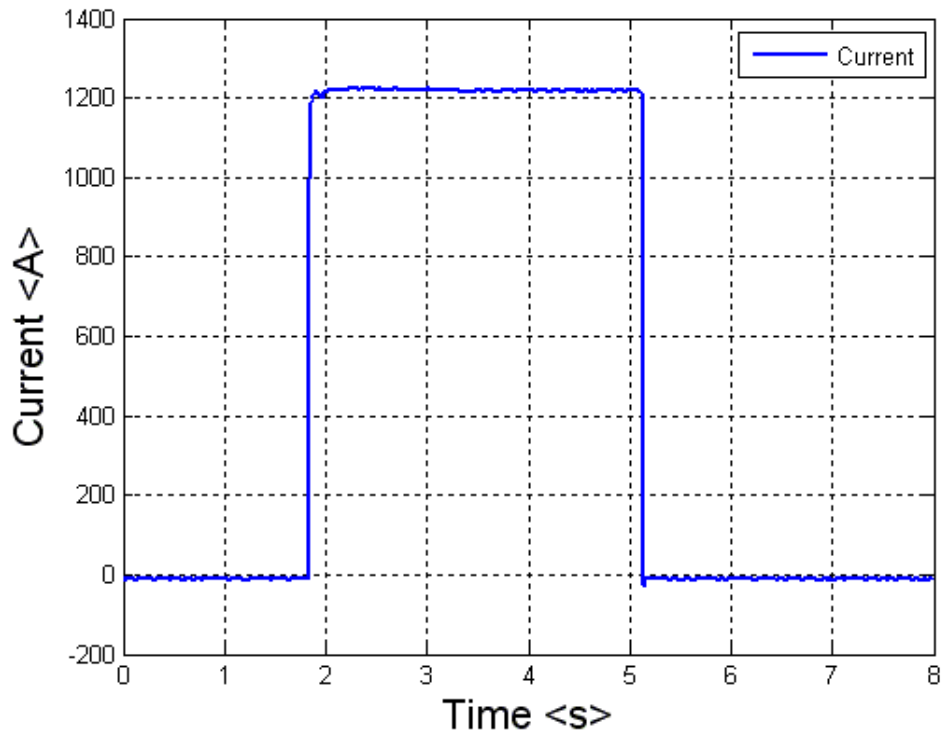


Figure 18. Armature Lorentz force and rail recoil force for 1.2 kA pulse

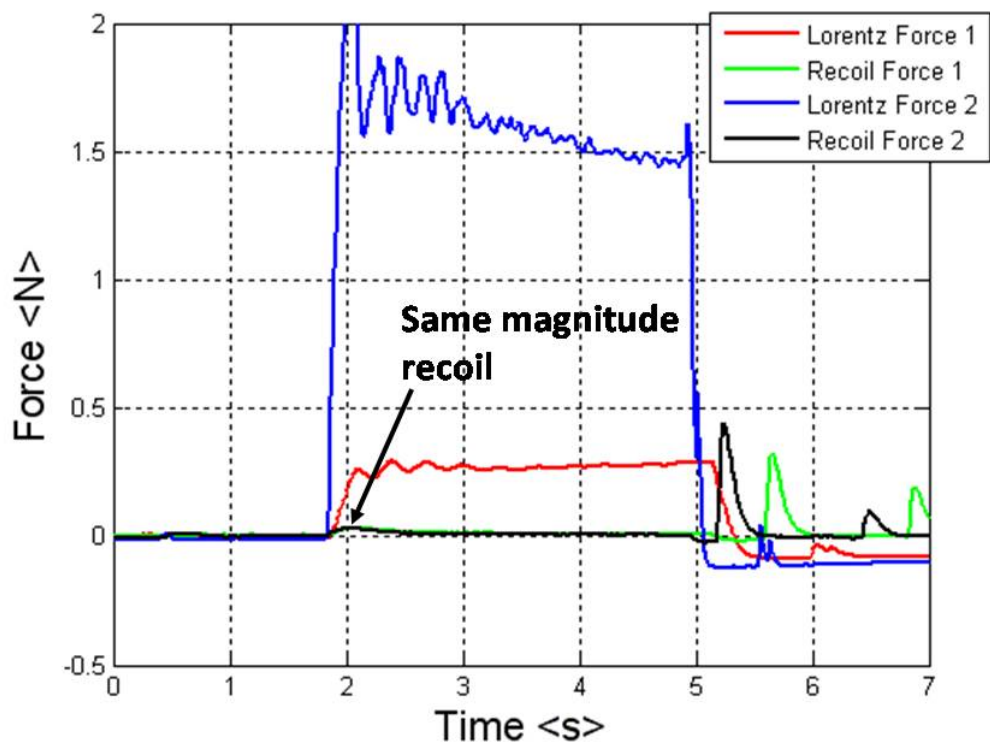
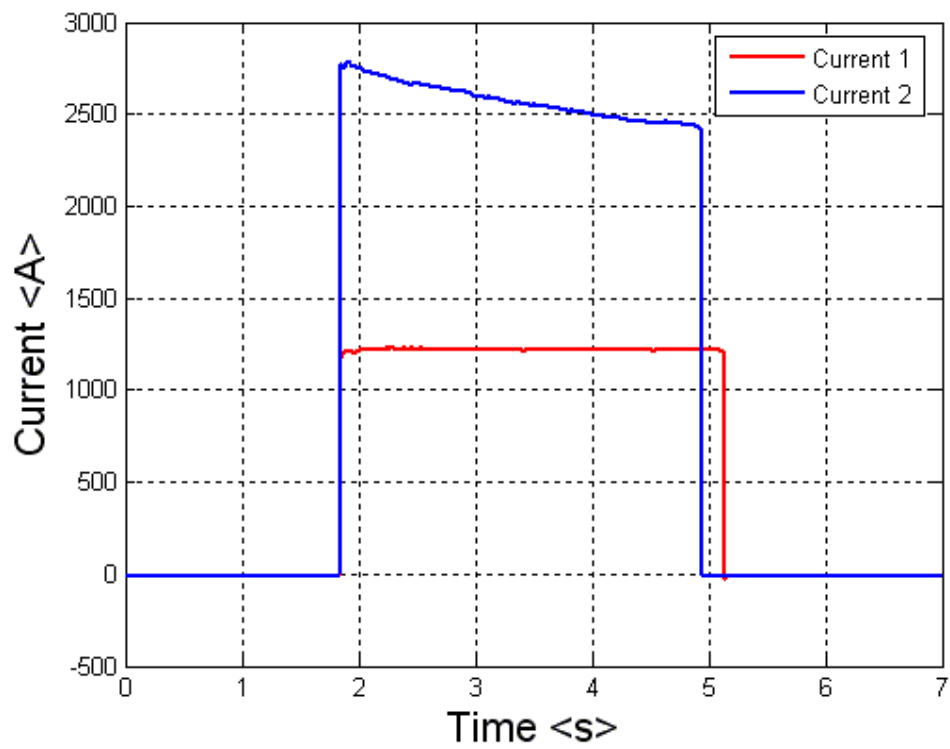


Figure 19. Armature Lorentz forces and rail recoil forces for 1.2 kA and 2.5 kA pulses

Tables 1 and 2 show how little the peak and steady-state rail recoil changed, regardless of the current and armature Lorentz force readings. The Lorentz force column refers to the force on the armature.

Current (A)	Lorentz Force (N)	Recoil Force-Peak (N)
857.8	0.18	0.036
1218.0	0.29	0.036
1539.3	0.443	0.036
1715.6	0.60	0.024
1849.7	0.72	0.034
2604.9	2.24	0.038
2683.8	2.64	0.030
2741.7	2.70	0.032

Table 1. Peak rail recoil force measurements

Current (A)	Lorentz Force (N)	Recoil Force- Steady State (N)
863.7	0.17	0.0039
1218.0	0.29	0.0098
1503.8	0.46	0.0106
1681.0	0.59	0.0063
1779.4	0.66	0.0086
2017.3	0.92	0.0083
2235.1	1.23	0.0078
2373.5	1.40	0.0119
2602.7	1.73	0.0102

Table 2. Steady-state rail recoil forces

The data in Table 2 is plotted in Figure 20. The Lorentz force on the armature is directly proportional to the square of the current while the recoil doesn't show consistent or predictable current dependence. The measured armature force is consistent with Equation (1). The steady-state force for each data point measures approximately 0.01 N, or less. The complete real-time graph for each data point can be viewed in Appendix section 1.

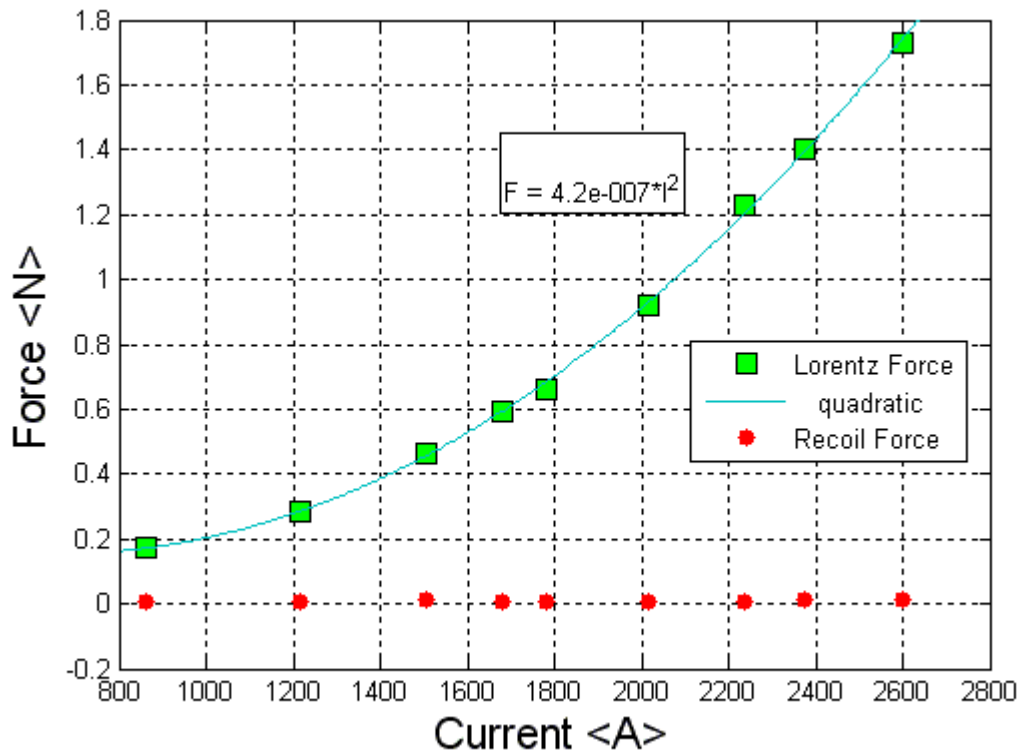


Figure 20. Armature Lorentz force and steady state rail recoil vs. current

B. SPLIT RAIL MEASUREMENTS

1. Armature Lorentz Force and Recoil on the Muzzle Half Rail

Results of the force comparison between armature Lorentz force and rail recoil did not change for the muzzle half of the rails once they were split. Figure 21 shows a nearly 2 kA current pulse and the forces measured. Results for other current levels can be view in Appendix section 2. During brief transient oscillations, as the circuit energized, the recoil peaked at 0.05 N, which is approximately 2% of the magnitude of the armature Lorentz force produced. After the transient, the steady-state recoil measured less than 0.01 N, which is less than 1% of the armature Lorentz force measured.

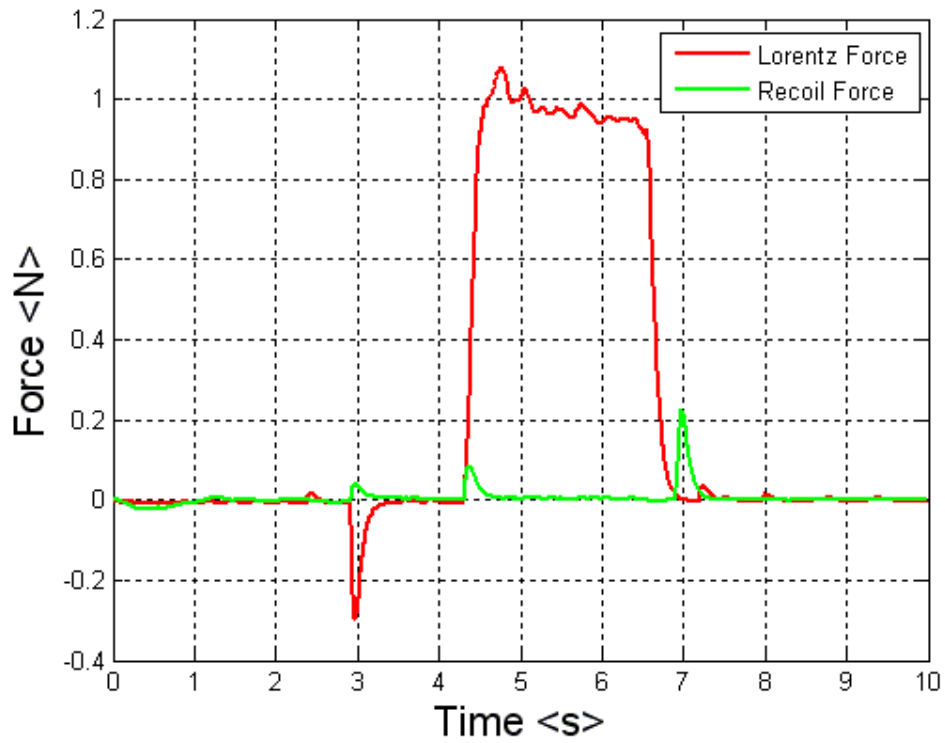
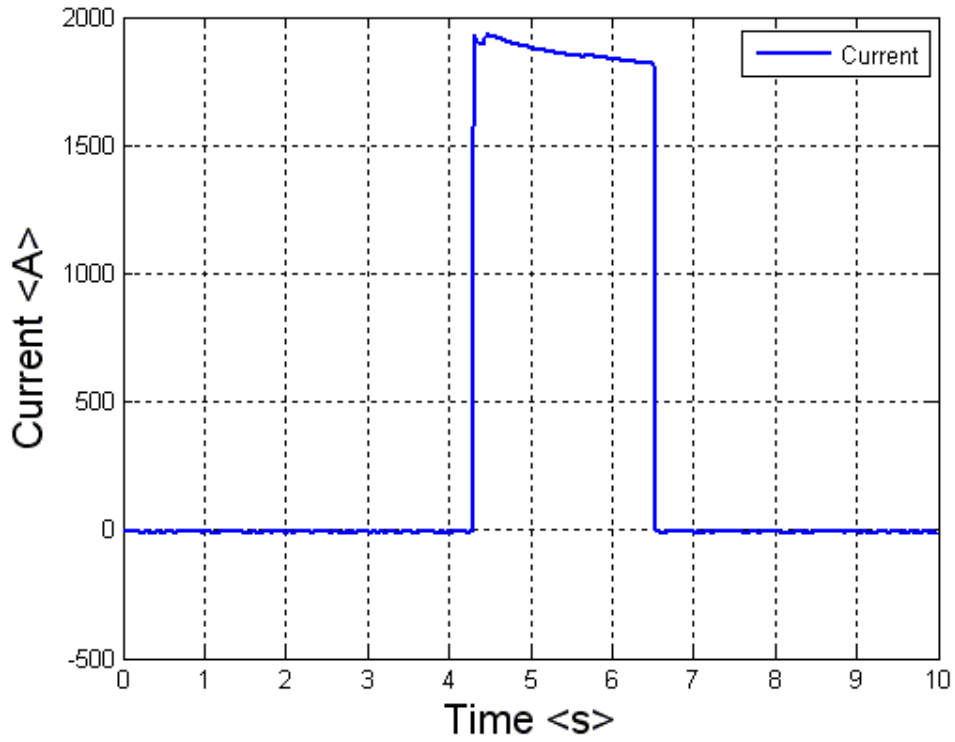


Figure 21. Split rails-armature Lorentz force and rail recoil force for 1.8 kA pulse

2. Forces Between the Rail Halves

Before the rails were split, it was evident that there was no net force on the rails. Splitting the rails was necessary to determine if there were equal and opposite forces being exerted on the rails. If recoil were seated in the rails and a canceling force from the breach region existed, then the rail halves would push together toward the center of the rails. Instead, the rails were found to push apart slightly. Figure 22 shows a 2 kA current pulse and equal and opposite forces of approximately 0.22 N being exerted on the rails. From separate measurements, similar current pulses created a Lorentz force of approximately 1 N. With the creation of two more sets of tabs dipped into eutectic, undesired vertical current components were introduced and the interactions of these with magnetic fields would exert forces separating the two halves of the rails. If one-dimensional current could have been achieved while splitting the rails, the author believes these opposing forces would not have existed. Furthermore, these equal and opposite forces are not believed to exist as internal stress within unbroken rails.

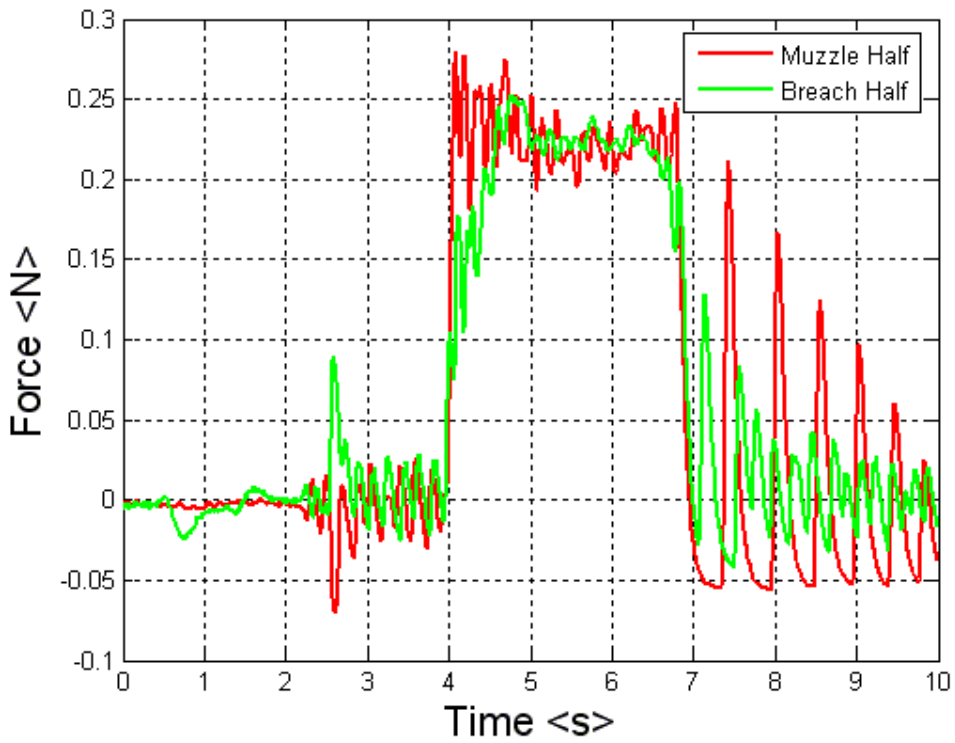
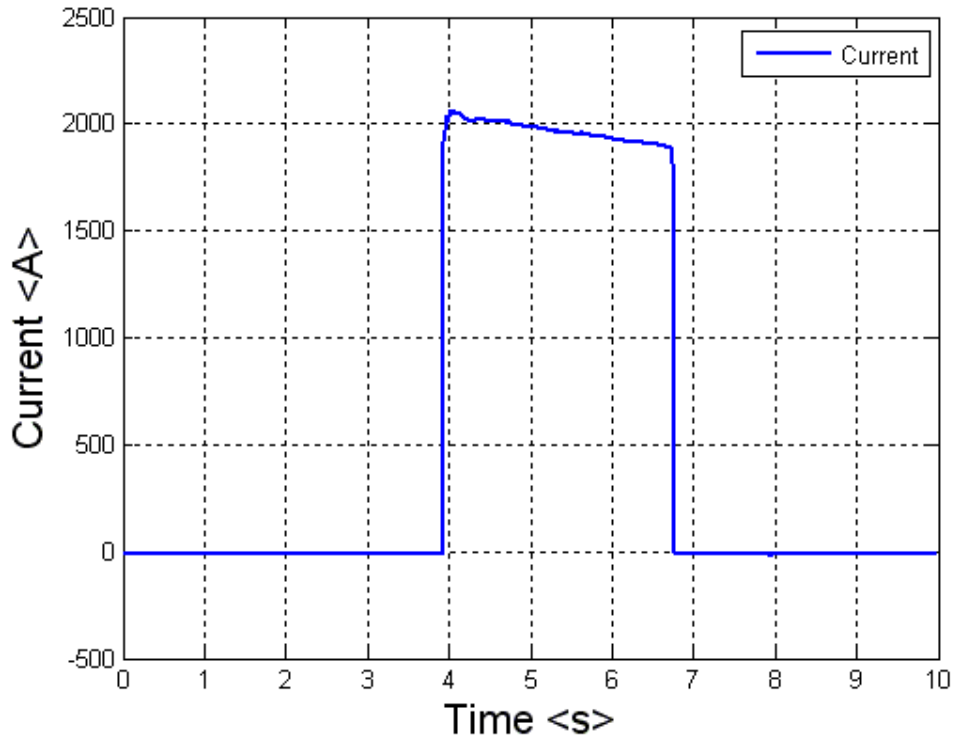


Figure 22. Split rail – Opposing rail forces for 2 kA current pulse

C. SUMMARY

An efficient and effective electromagnetic railgun design rests on a thorough understanding of the forces at work within the gun. The research in this thesis addresses the controversial question, "Are recoil forces seated in the rails?" This question impacts how the gun should be designed, and what resources would be needed. The weight, size, and durability will be among the primary concerns when EM railguns are installed on ships.

This experiment investigated recoil exerted on the rails by simultaneously measuring armature Lorentz force and rail recoil with real-time data recording. If the recoil was seated in the rails, it was expected to have a magnitude nearly equal to the Lorentz force in the opposite direction. Simultaneous measurements over a large range of currents were compared. The max current attained was 2.7 kA, and the measured Lorentz force was 1.7 N, while the recoil peaked at less than 2% of this value and then dropped to less than 1%, as seen in Figure 19. Appendix section 1 shows graphical results for various current levels, which are consistent with the results in Figure 19. The recoil readings are not current dependent, and are interpreted as artifacts of the experiment.

Splitting the rails and simultaneously measuring armature Lorentz force and recoil on the muzzle half of the rails yielded results consistent with those for the unsplit rails. The maximum current attained with this setup was 1.9 kA, and the measured Lorentz force was approximately 1 N, while the steady-state recoil was less than 1% of this value, as seen in Figure 21. The equal and opposite forces

pushing the split rails apart in Figure 22 are interpreted as an artifact of the experiment, and are not associated with recoil in any way. The fact that the split rails did not push toward each other, combined with the results from the split rail Lorentz-recoil measurements (Figure 21), leads to the conclusion that there are not any internal stresses within the rails.

Since there are no indications of internal stresses and the simultaneous Lorentz-recoil measurements do not indicate a Lorentz reaction force on the rails, this experimental investigation has shown that recoil forces are not seated in the rails.

APPENDIX

1. LORENTZ FORCE AND RECOIL

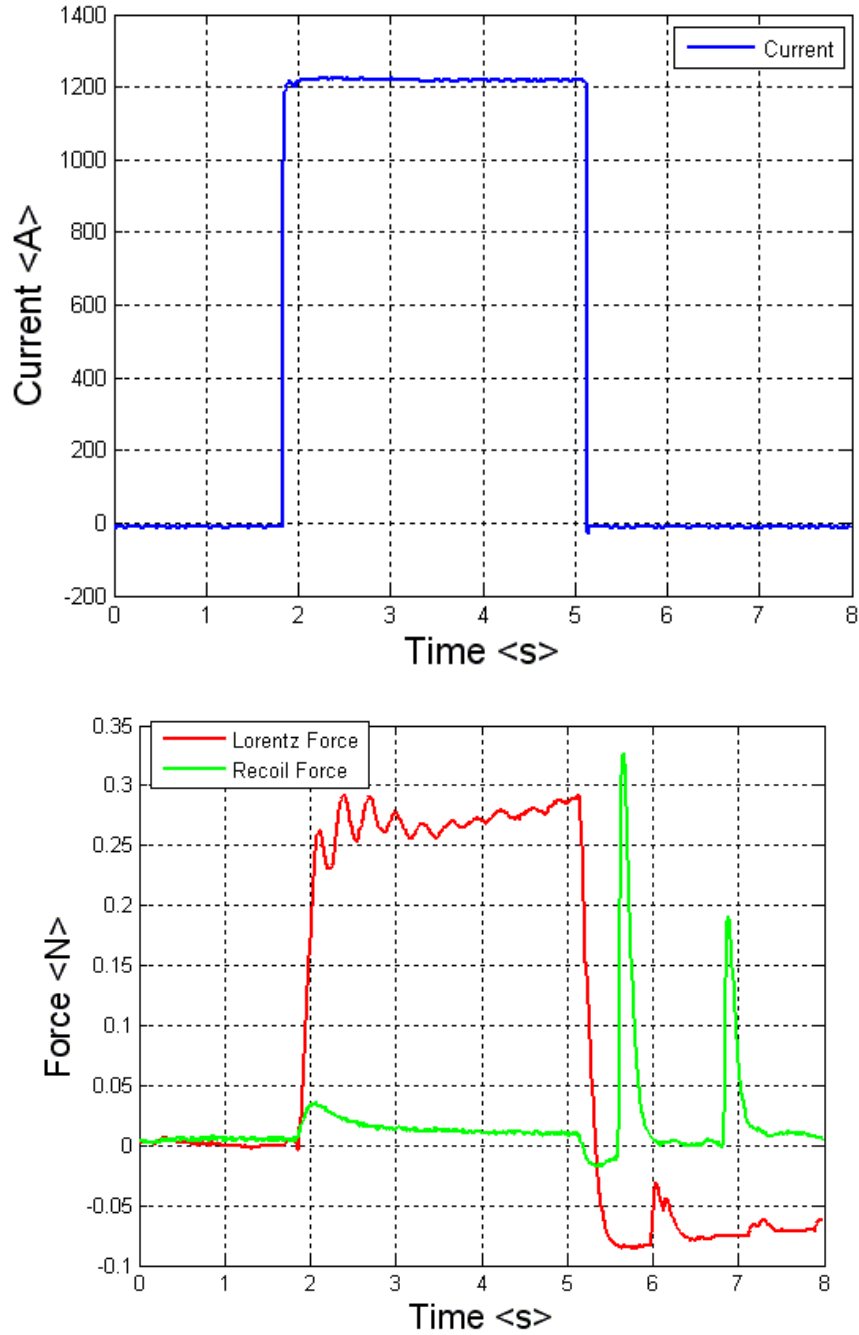


Figure 23. Armature Lorentz force and rail recoil force for 1.2 kA pulse

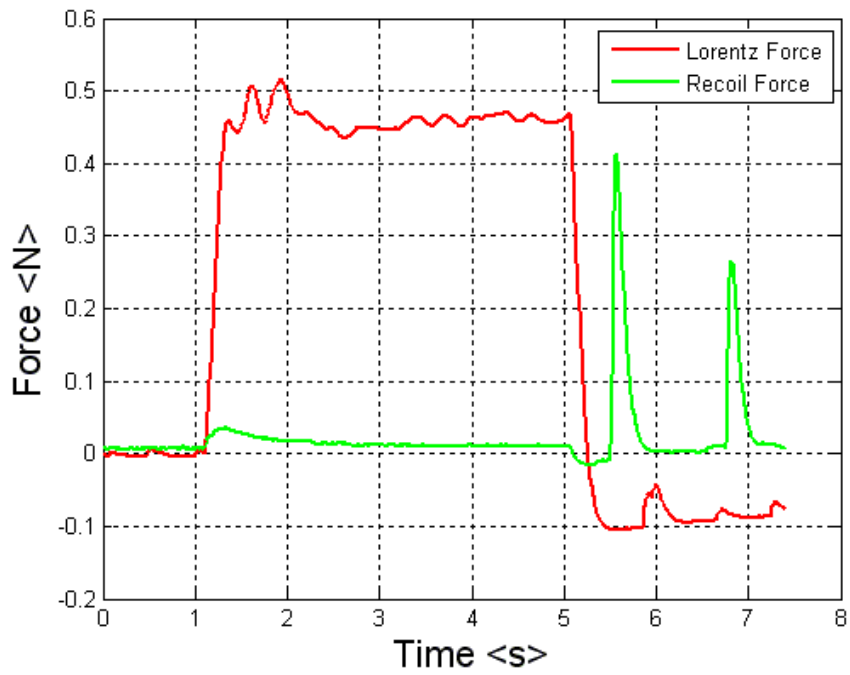
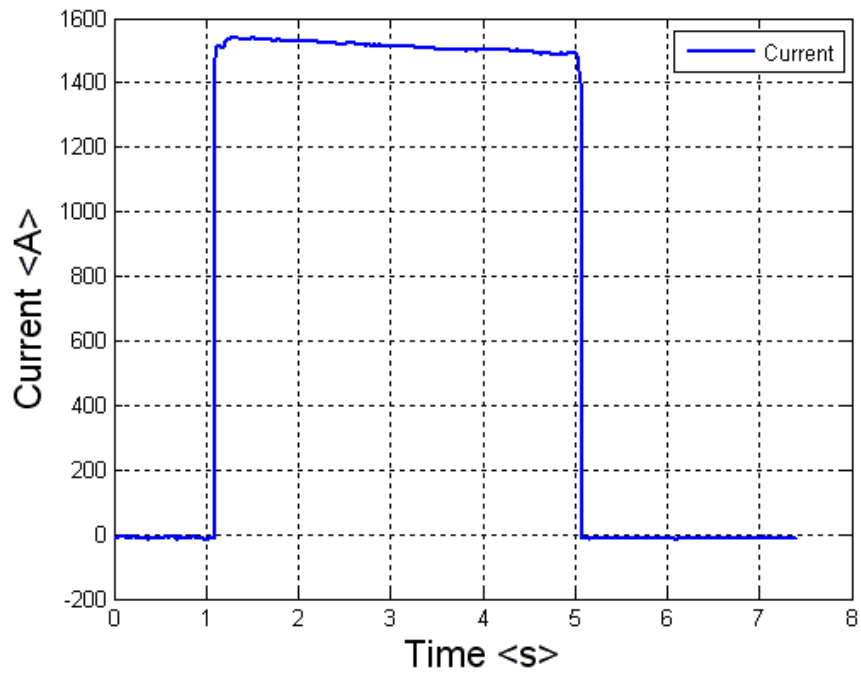


Figure 24. Armature Lorentz force and rail recoil force for 1.5 kA pulse

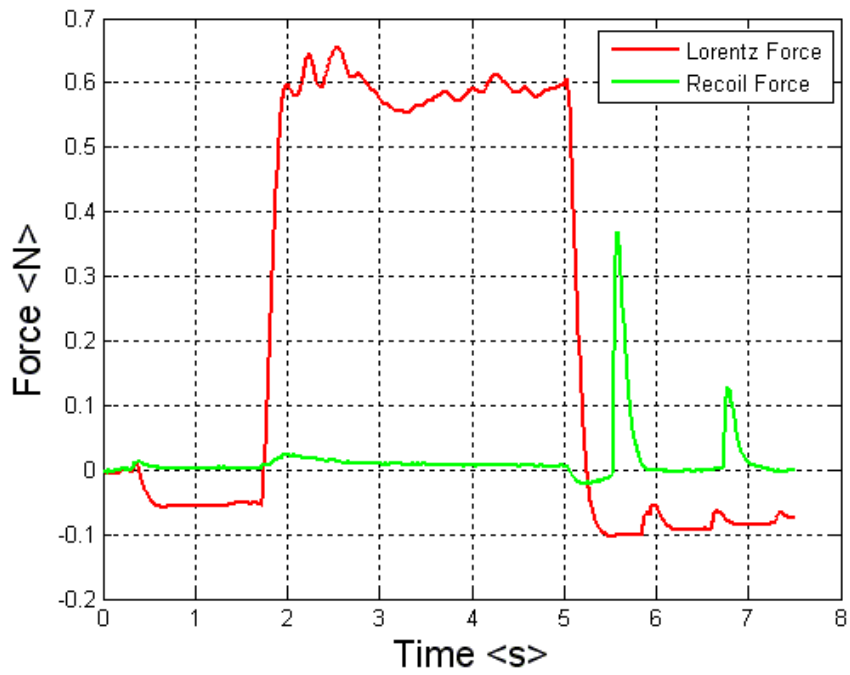
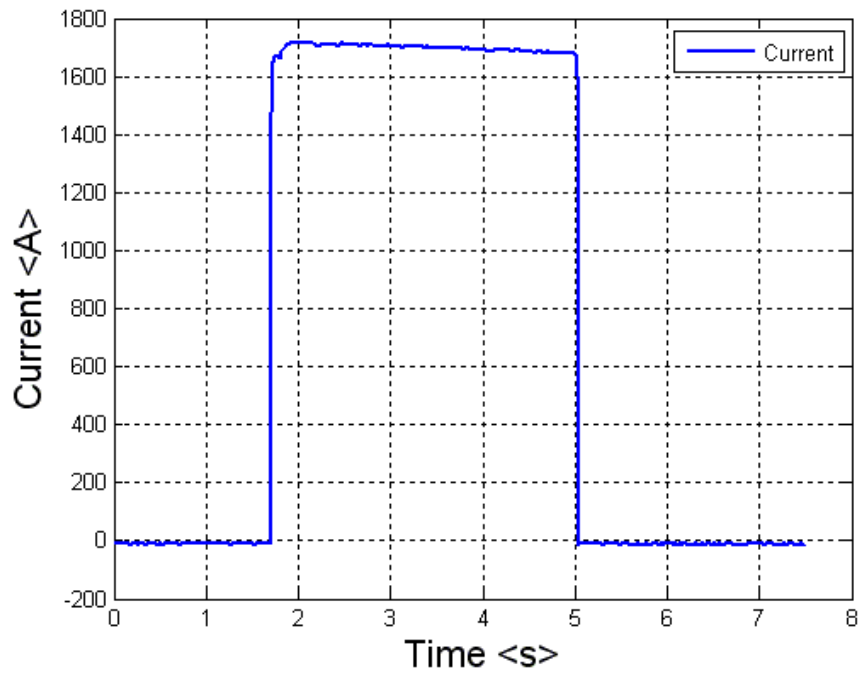


Figure 25. Armature Lorentz force and rail recoil force for 1.7 kA pulse

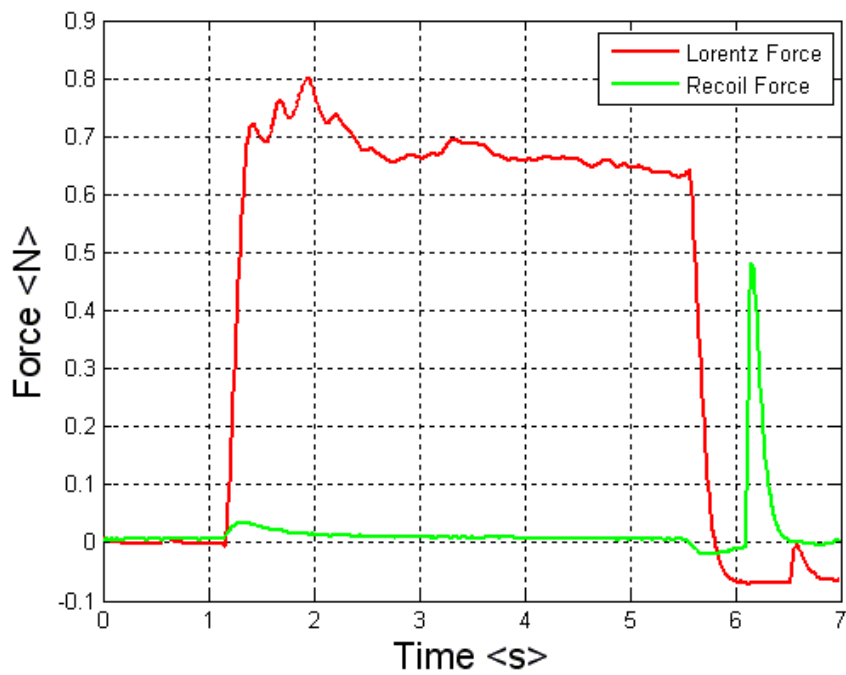
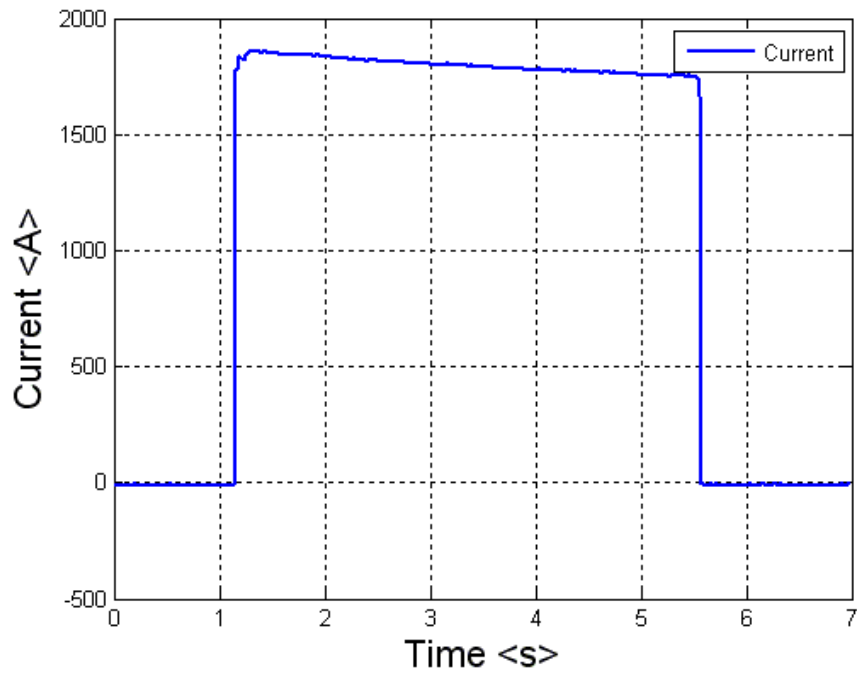


Figure 26. Armature Lorentz force and rail recoil force for 1.8 kA pulse

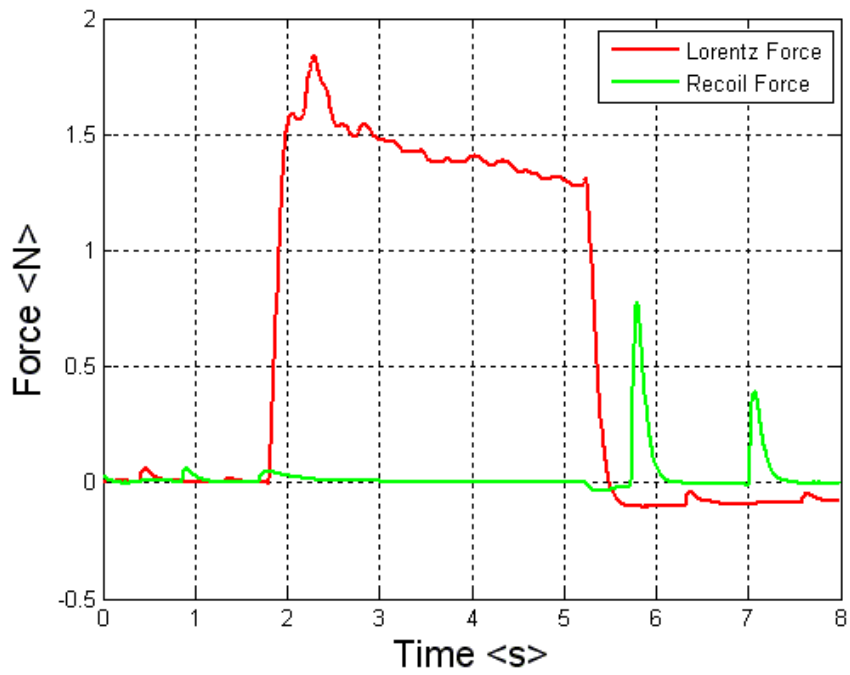
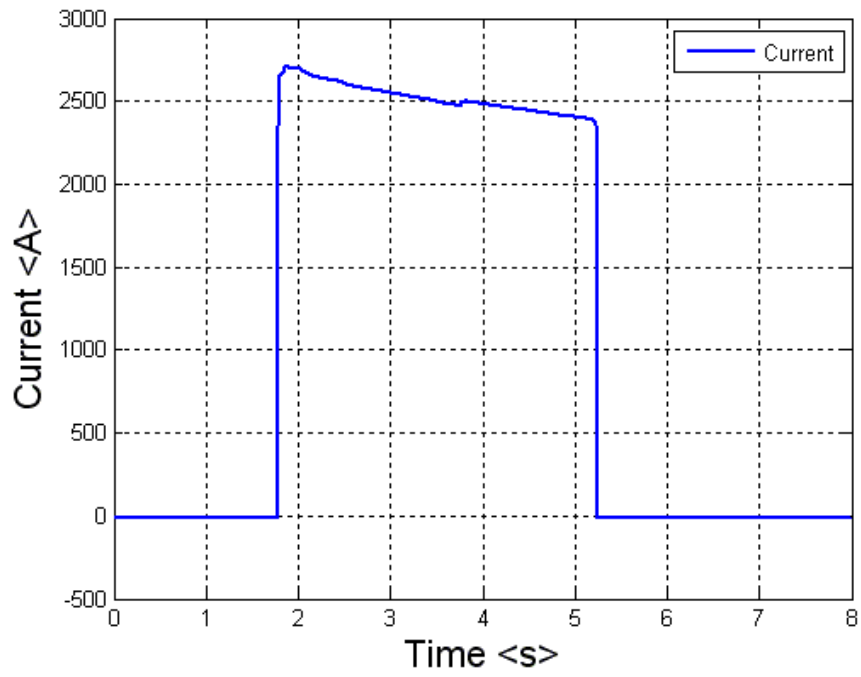


Figure 27. Armature Lorentz force and rail recoil force for 2.6 kA pulse

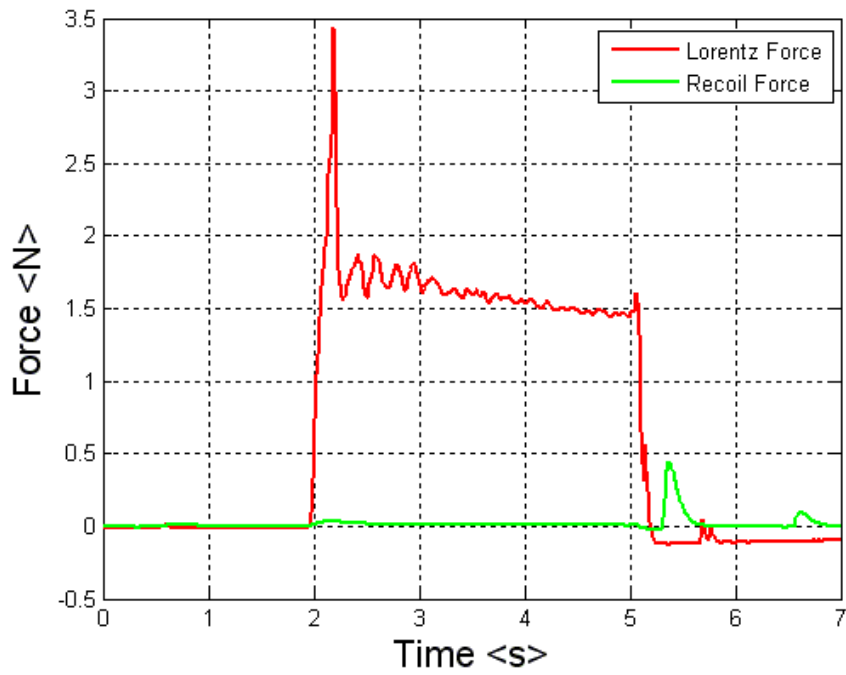
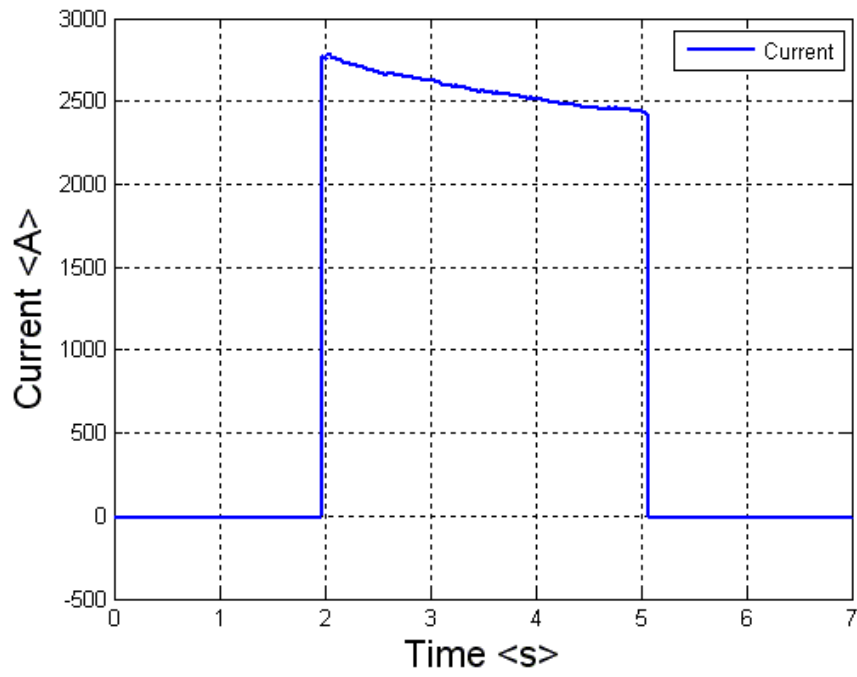


Figure 28. Armature Lorentz force and rail recoil force for 2.7 kA pulse

2. SPLIT RAILS—LORENTZ FORCE AND MUZZLE HALF RECOIL

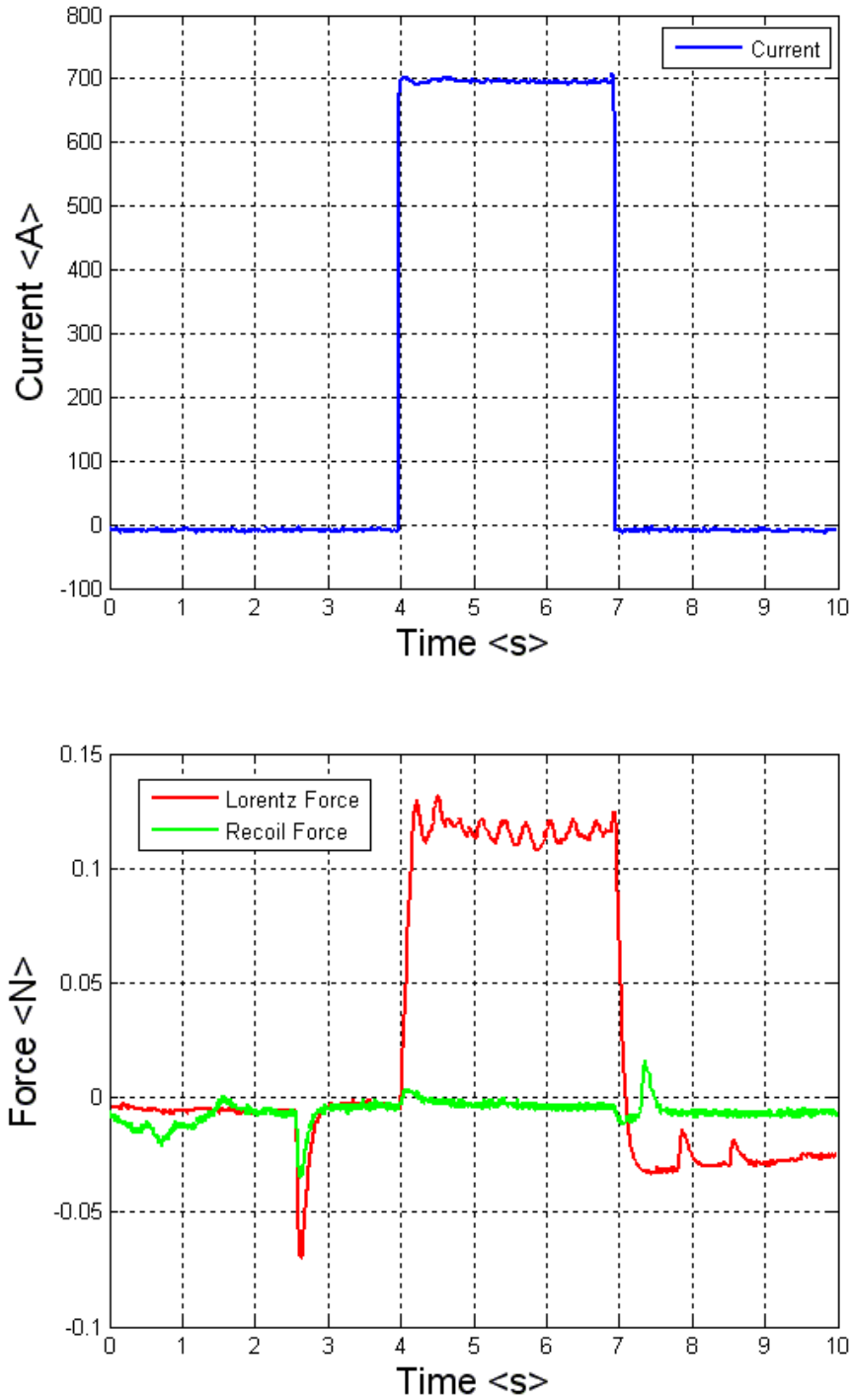


Figure 29. Split rail – armature Lorentz force and recoil force for 0.7 kA pulse

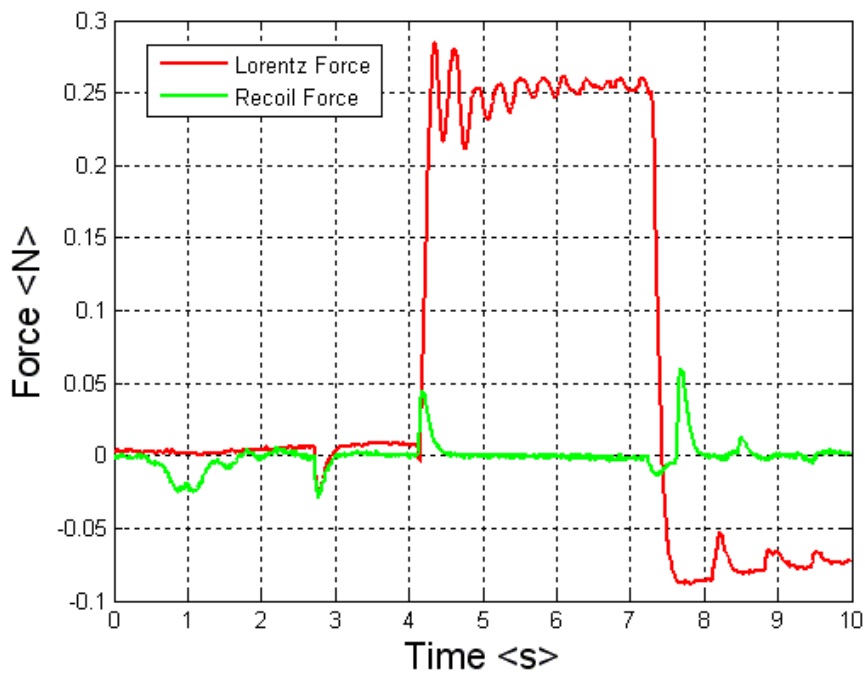
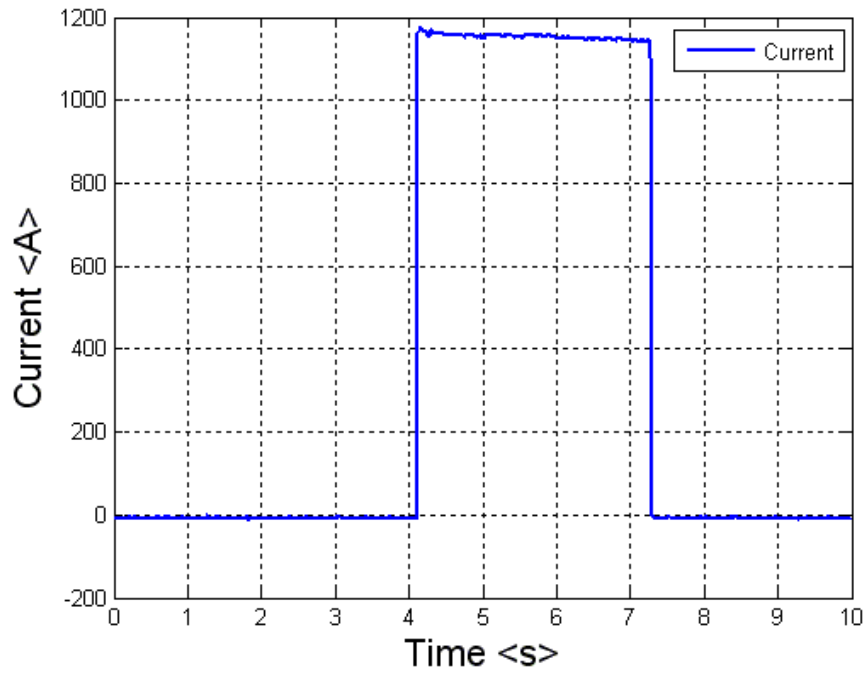


Figure 30. Split rail – armature Lorentz force and recoil force for 1.2 kA pulse

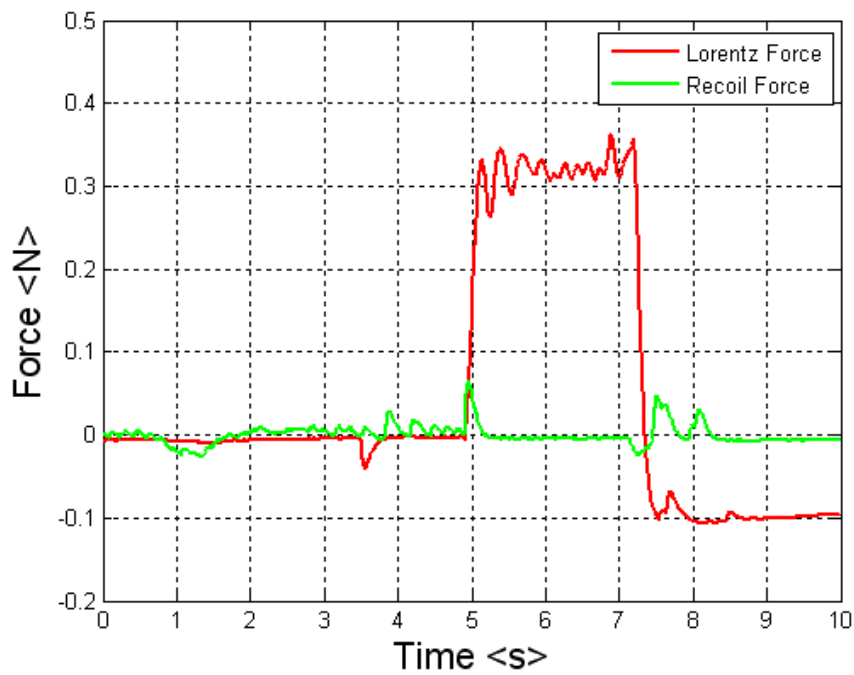
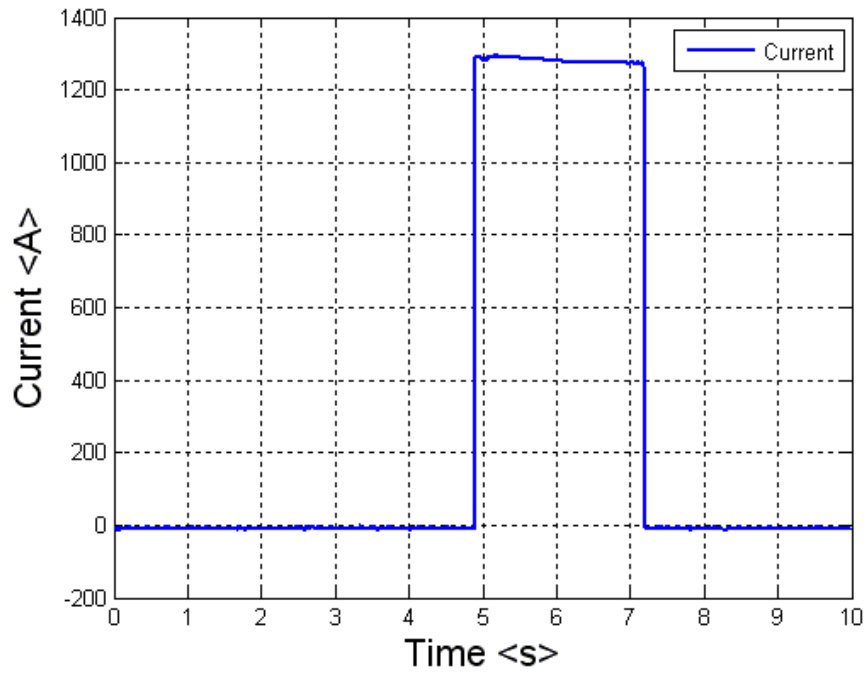


Figure 31. Split rail – armature Lorentz force and recoil force for 1.3 kA pulse

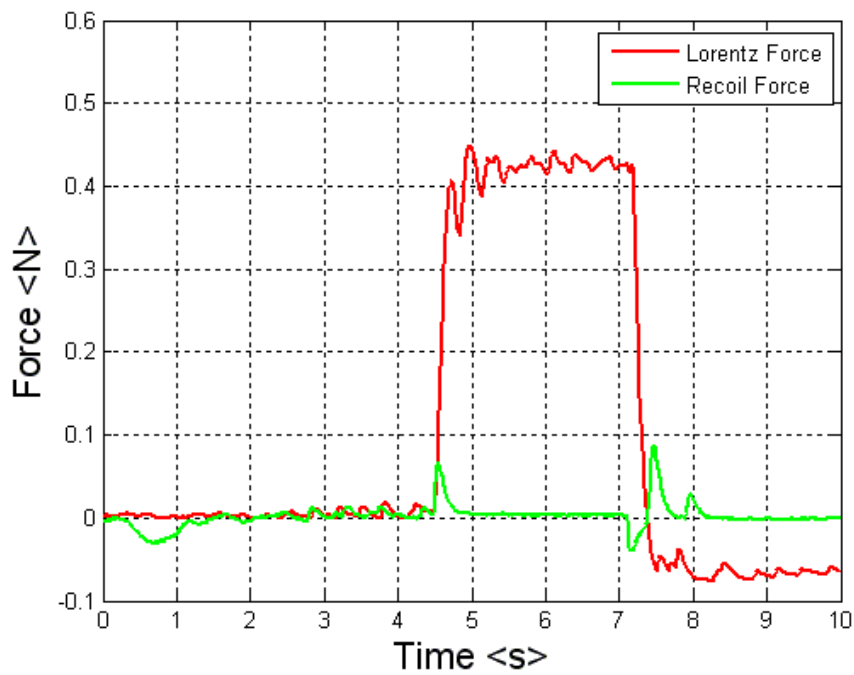
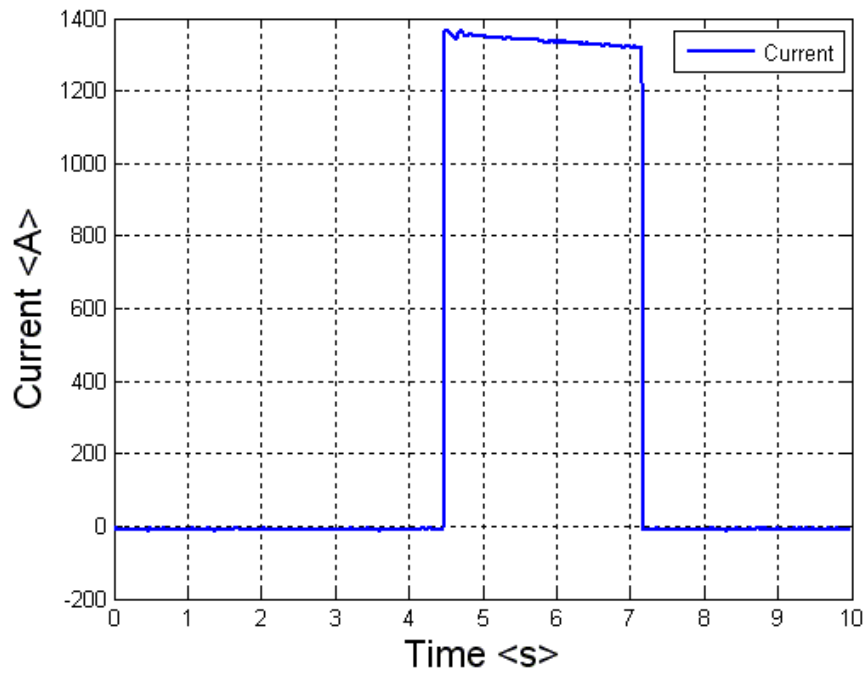


Figure 32. Split rail – armature Lorentz force and recoil force for 1.3 kA pulse

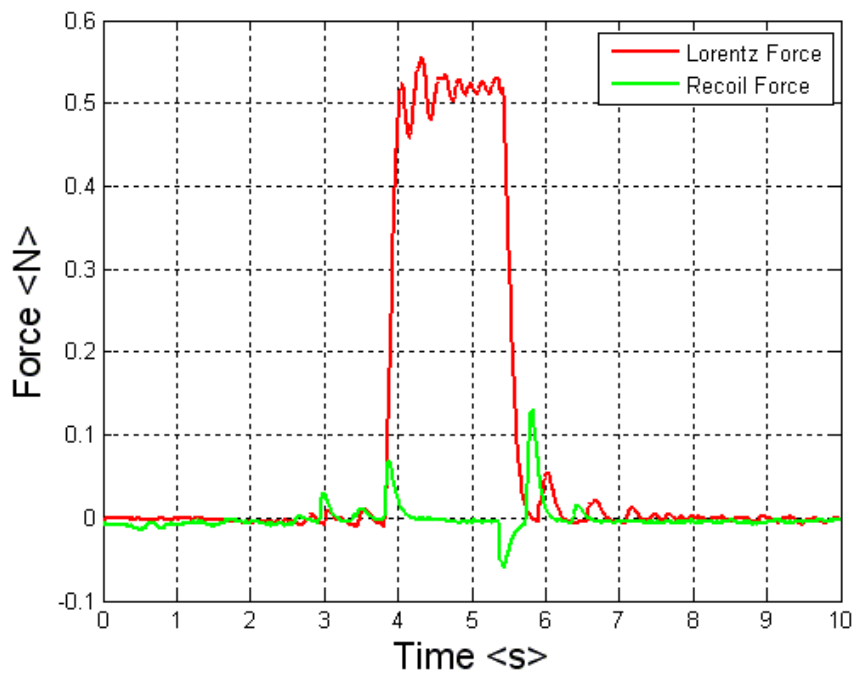
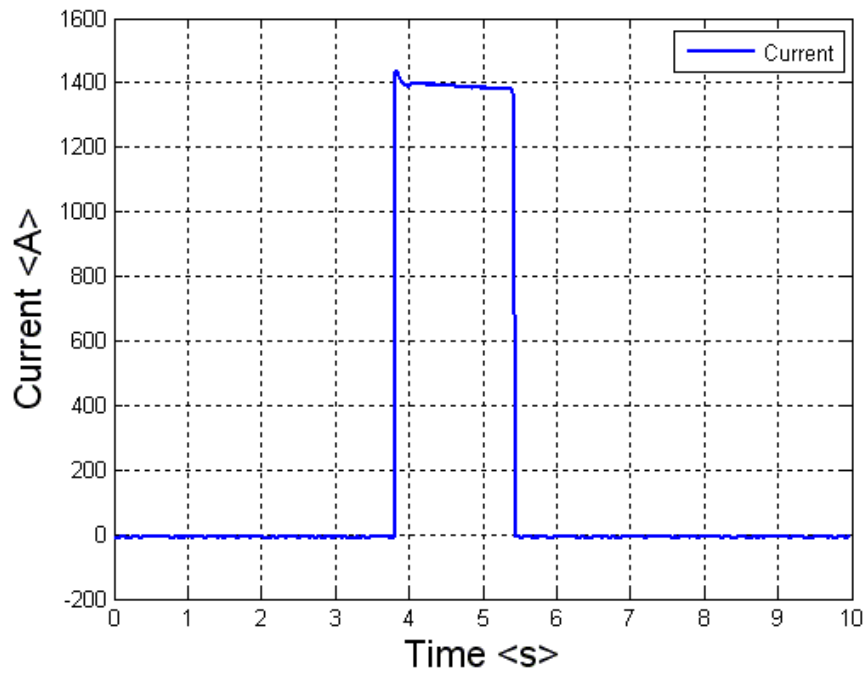


Figure 33. Split rail – armature Lorentz force and recoil force for 1.4 kA pulse

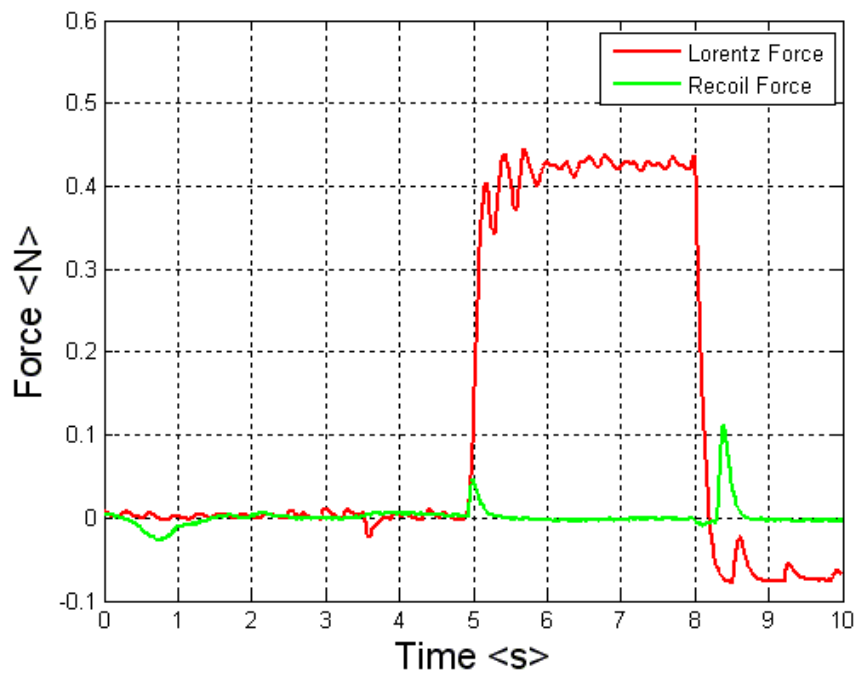
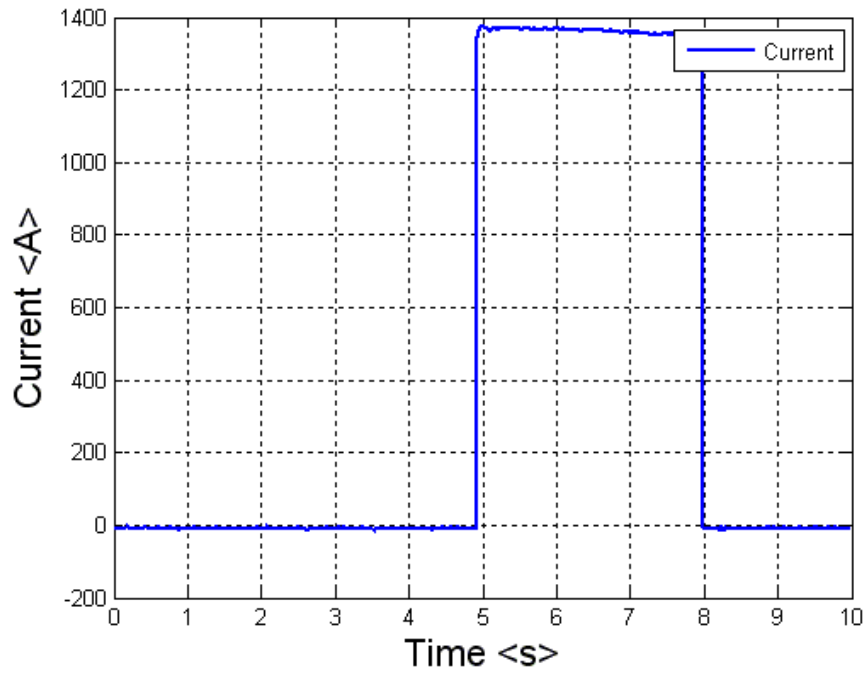


Figure 34. Split rail – armature Lorentz force and recoil force for 1.4 kA pulse

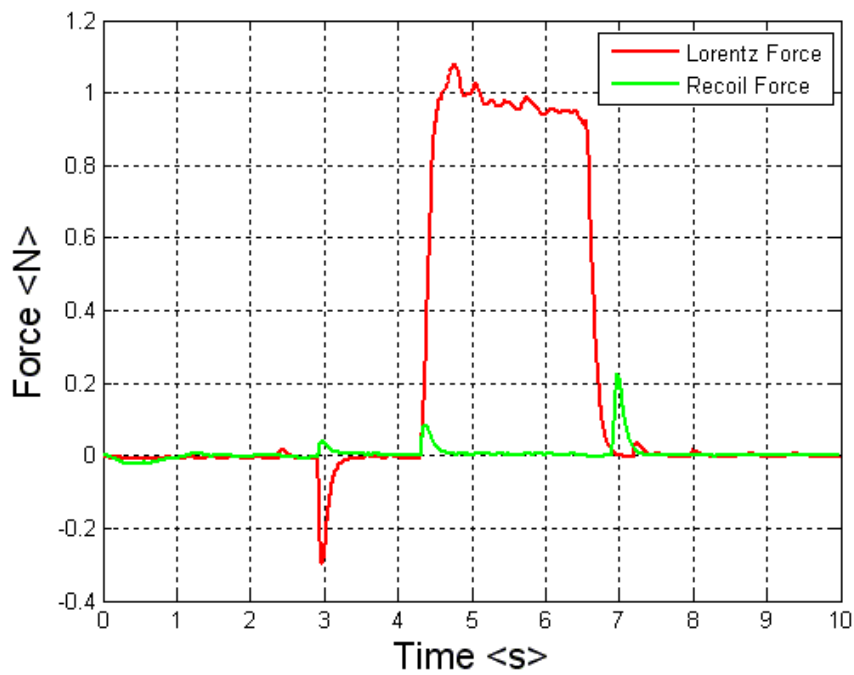
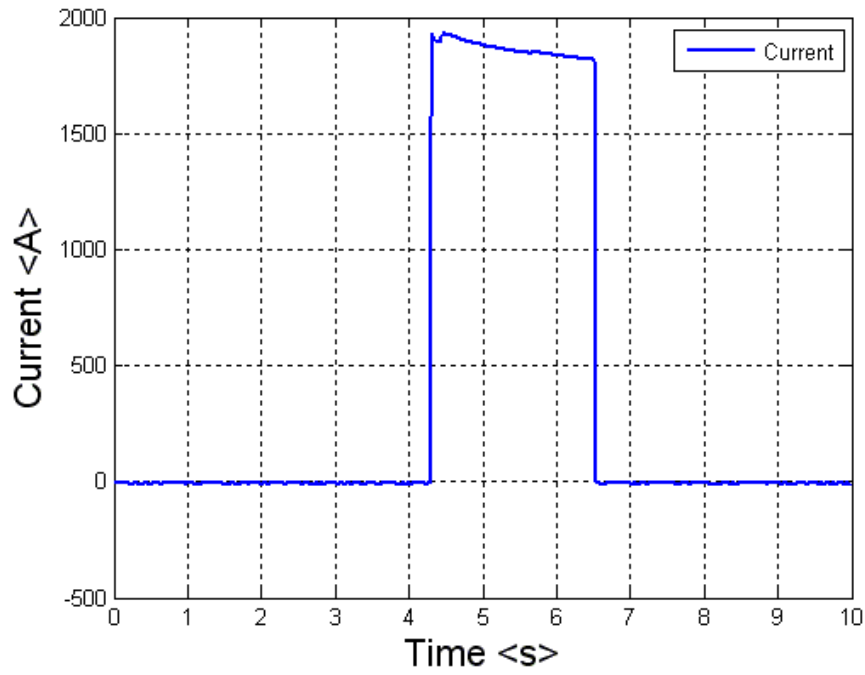


Figure 35. Split rail – armature Lorentz force and recoil force for 1.9 kA pulse

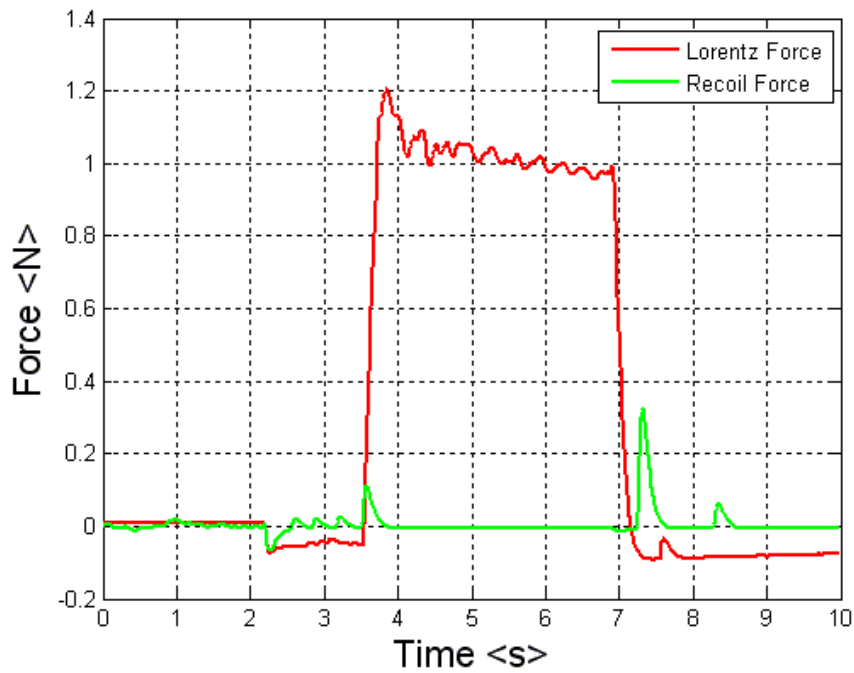
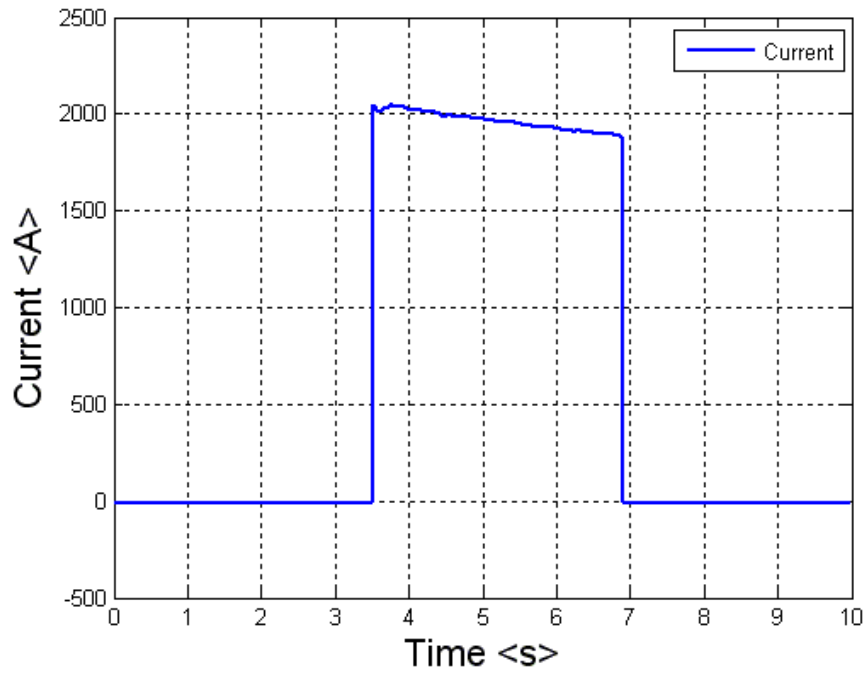


Figure 36. Split rail – armature Lorentz force and recoil force for 2 kA pulse

3. SPLIT RAILS—OPPOSING FORCES ON EACH RAIL HALF

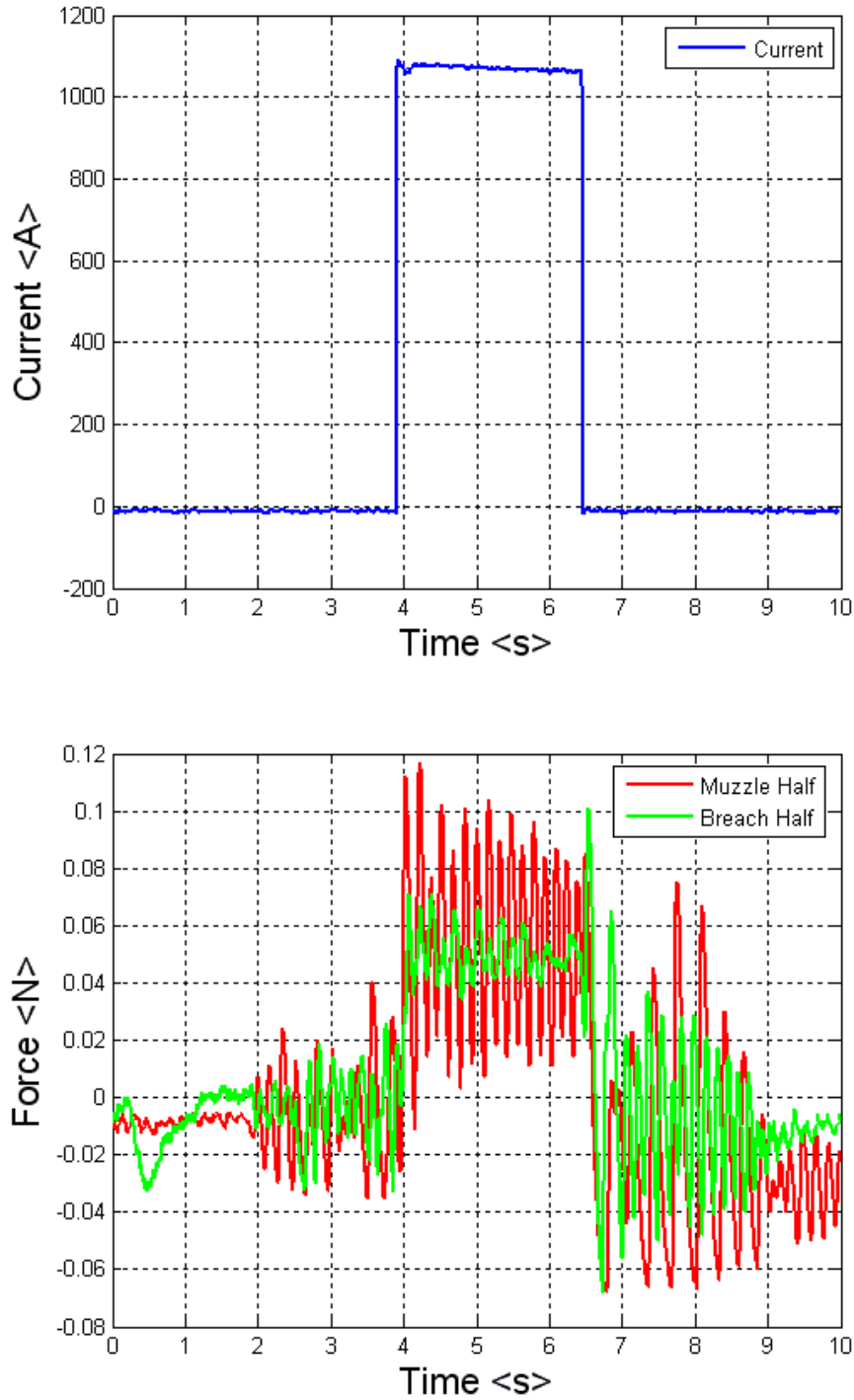


Figure 37. Split rail – opposing rail forces for 1.1 kA current pulse

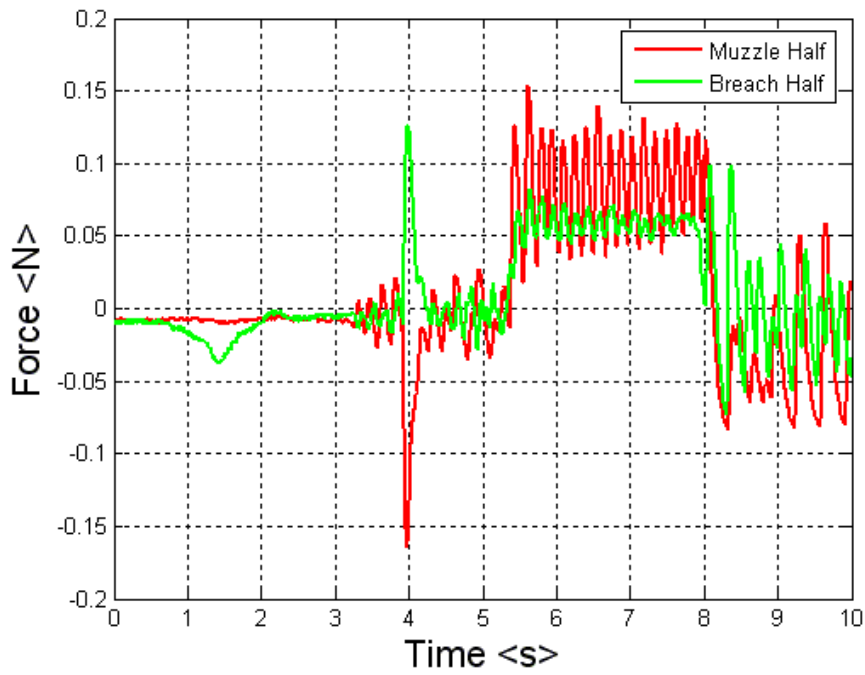
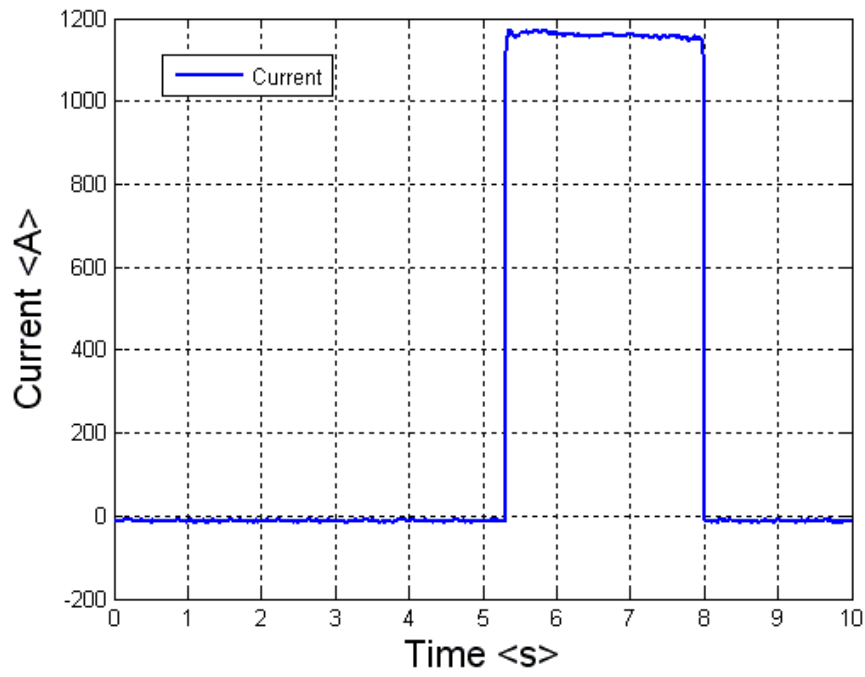


Figure 38. Split rail – opposing rail forces for 1.2 kA current pulse

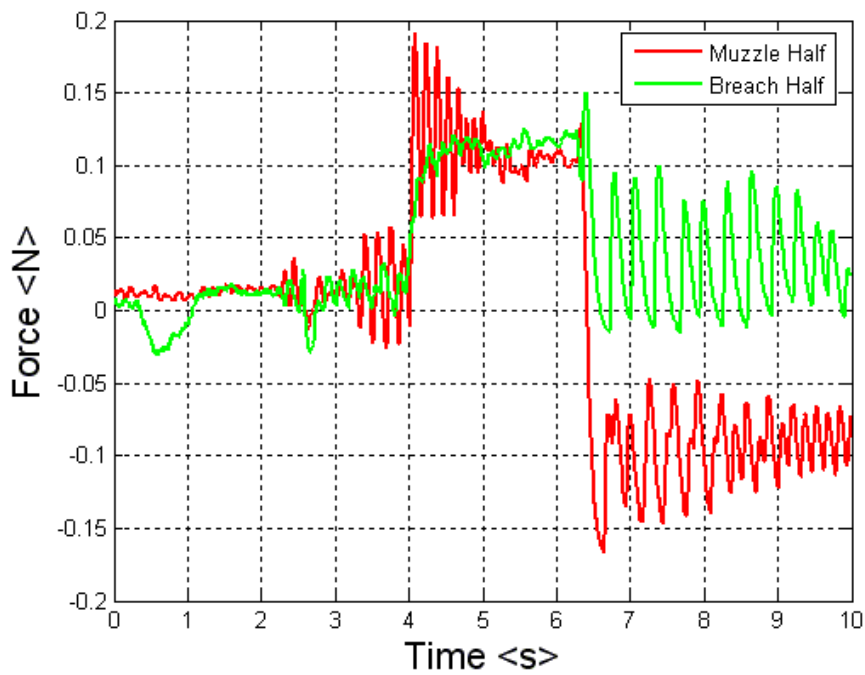
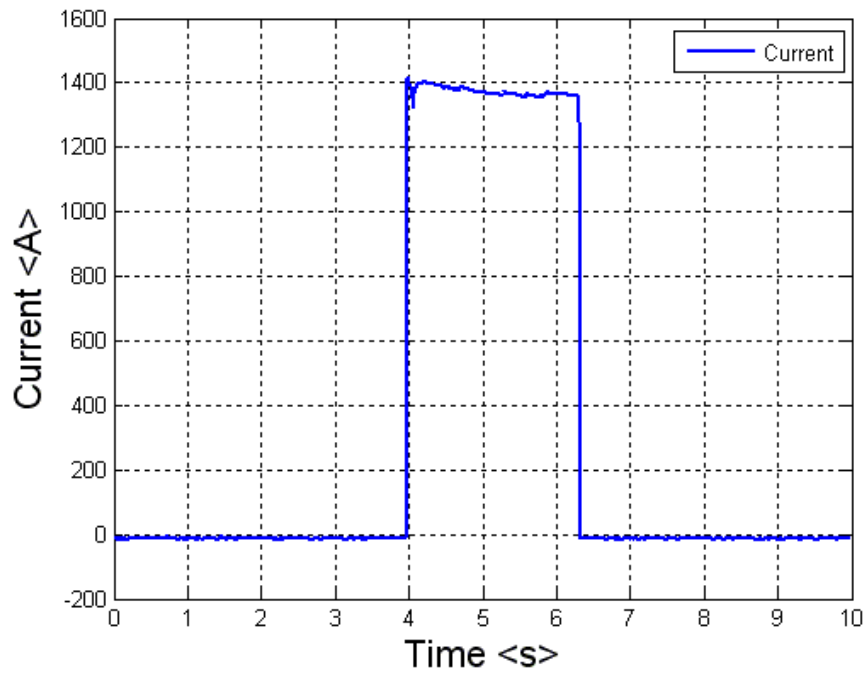


Figure 39. Split rail – opposing rail forces for 1.4 kA current pulse

THIS PAGE INTENTIONALLY LEFT BLANK

LIST OF REFERENCES

- [1] S. Sandro and R. Wilson, "Romagnosi and the discovery of electromagnetism," *Accademia dei Lincei*, Series 9, volume 11, issue 2, pp. 137-142, 2000.
- [2] "Hans Christian Ørsted," *Encyclopedia Britannica Online*,
<http://www.britannica.com/EBchecked/topic/433282/Hans-Christian-Orsted> (accessed November 20, 2009).
- [3] I.V. Hogg, *The Guns: 1939/45*. London: Macdonald and Co., 1969.
- [4] O. Darrigol, *Electrodynamics from Ampère to Einstein*, Oxford, [England]: Oxford University Press, 200, p. 327.
- [5] I.E. Allen and T.V. Jones, "Relativistic recoil and the railgun," *J. App. Phys.*, volume 67, pp. 18-21, 1990.
- [6] J. E. Allen, "Railgun recoil and relativity" *J. Appl. Phys.*, volume 20, pp. 1073, 1987.
- [7] H. Aspden, "The exploding wire phenomenon," *Physics Letters*, volume 107A, pp. 238-240, February 1985.
- [8] T. H. Boyer, "Energy and momentum in electromagnetic field for charged particles moving with constant velocities," *Am. J. Phys.*, volume 39, pp. 257-270, March 1971.
- [9] B. R. Casserberg, "Electromagnetic momentum introduced simply," *Am. J. Phys.*, volume 50, pp. 415-416, May 1982.
- [10] P. Graneau and P. N. Graneau, "Electrodynamic momentum measurements," *J. Phys. D: Appl. Phys.*, volume 21, p. 1826, 1988.
- [11] P. Graneau and N. Graneau, "The electromagnetic impulse pendulum and momentum conservation," *Nuovo Cimento*, volume 7D, pp. 31-45, 1986.

- [12] T. K. Hsieh, "A Lagrangian formulation for mechanically, thermally coupled electromagnetic diffusive processes with moving conductors," *IEEE Trans. Mag.*, volume 31, no. 1, 1995.
- [13] L. Johansson, "Longitudinal electrodynamic forces-and their possible technological applications," Master's thesis, Lund Institute of Technology, Lund Sweden, September 1996.
- [14] E. L. Kathe, "Recoil Considerations for Railguns," *IEEE Trans. Mag.*, volume 37, no 1, Part 1, pp. 425-430, January 2001.
- [15] M. Löffler, "Recoil forces in electromagnetic accelerators-A short review," in *Proc. 4th Euro. Symp. Electromagn. Launch Technol.*, Celle, Germany, May 1993.
- [16] R. A. Marshall and L. C. Woods, "Comment: Origin, location, magnitude and consequences of recoil in the plasma armature railgun," *Inst. Elect. Eng. Proc. Sci. Meas. Technol.*, volume 144, pp. 49-51, 1997.
- [17] P. G. Moyssides, "Pendulum Experiments and the Fundamental Laws of Electrodynamics," *Inst. Elect. Eng. Proc. Sci. Meas. Technol.*, volume 35, no. 2, March 1999.
- [18] P. Graneau and N. Graneau, "Railgun Recoil Forces Cannot Be Modeled as Gas Pressure," *IEEE Trans. Magn.*, volume 33 no. 6, p. 18, 1997.
- [19] M. Pollack and L. W. Matsch, "Electric gun and power source," *Armour Research Foundation Report No. 3, Project 15-391E*, May 1, 1947.
- [20] A. E. Robson and J. D. Sethian, "Railgun recoil, ampere tension, and the laws of electrodynamics," *Am. J. Phys.*, volume 60, pp. 1111-1117, December 1992.
- [21] J. J. G. Scanio, "Conservation of momentum in electrodynamics-an example," *Am. J. Phys.*, volume 43, pp. 258-260, March 1975.

- [22] D. Sadedin, "Conservation of Momentum and Recoil in the Railgun," *IEEE Trans*, volume 33 no. 1, pp. 599-603, 1997.
- [23] J. G. Ternan, "Equivalence of the Lorentz and Ampere force laws in magnetostatics," *J. Appl. Phys.*, volume 57, pp. 1743-1745, 1985
- [24] W. Weldon, M. Driga, and H. Woodson, "Recoil in Electromagnetic Railguns," *IEEE Trans*, volume 22 no. 6, pp. 1808-1811, November 1986.
- [25] J. P. Wesley, "On Peoglos' measurement of the force on a portion of a current loop due to the remainder of the loop," *J. Phys. D: Appl. Phys.*, volume 22, pp. 849-850, 1989.
- [26] A. E. Witalis, "Origin, location, magnitude and consequences of recoil in the plasma armature railgun," *Inst. Elect. Eng. Proc. Sci. Meas. Technol.*, volume 142, pp. 197-200, 1995.
- [27] P. Graneau, "Amperian recoil and the efficiency of railguns," *J. Appl. Phys.*, volume 62, pp. 3006-3009, 1987.
- [28] W.B. Maier, "Selected Topics in Railgun Technology" (revised September 3, 2008), Course Notes, Naval Postgraduate School, Monterey, CA, 2008.
- [29] R. Ellis, Technical Director, USN EM Railgun INP, Office of Naval Research, Arlington, VA.
- [30] M. Schroeder, "An investigation of the static force balance of a model railgun," Master's thesis, Naval Postgraduate School, Monterey, CA, 2007.

THIS PAGE INTENTIONALLY LEFT BLANK

INITIAL DISTRIBUTION LIST

1. Defense Technical Information Center
Ft. Belvoir, Virginia
2. Dudley Knox Library
Naval Postgraduate School
Monterey, California
3. William B. Maier II
Physics Department
Code PHMW
Naval Postgraduate School
Monterey, California
4. Railgun Research Group
Physics Department
Code PH
Naval Postgraduate School
Monterey, California
5. CAPT David Kiel
PMS 405
Naval Sea Systems Command
Washington Navy Yard
Washington, DC
6. Dr. Roger McGinnis
PMS 405
Naval Sea Systems Command
Washington Navy Yard
Washington, DC
7. Gene Nolting
PMS 405
Naval Sea Systems Command
Washington Navy Yard
Washington, DC
8. Fred Beach
Institute of Advanced Technology
University of Texas at Austin
Austin, Texas

9. Dr. Elizabeth D'Andrea
Director, Swampworks
Office of Naval Research
Arlington, Virginia
10. Bob Turman
Sandia National Laboratories, New Mexico
Albuquerque, New Mexico
11. Stephen Bayne
US Army Research Laboratory
Adelphi, Maryland
12. Ian McNab
Institute of Advanced Technology
University of Texas at Austin
Austin, Texas
13. Roger Ellis
Naval Sea Systems Command, Dahlgren
Dahlgren, Virginia
14. Matthew Cilli
ARDEC
Picatinny Arsenal
Picatinny, New Jersey
15. Edward Schmidt
ARDEC
Aberdeen Proving Ground
Aberdeen, Maryland
16. D. S. Sorenson
Los Alamos National Laboratory
Los Alamos New Mexico
17. Jack Bernardus
NSWC, Dahlgren
Dahlgren, Virginia.
18. Andres Larraza
Physics Department Chair
Naval Postgraduate School
Monterey, California

19. Prof. Hans Mark
Institute for Advanced Technology
Austin, Texas

20. Bruce Denardo
Physics Department
Naval Postgraduate School
Monterey, California